ผลของการใช้มีเซนไคมอลสเต็มเซลล์ร่วมกับโครงร่างเซลล์เชิงประกอบระหว่างพอลิคาโพรแลคโตน/ไฮดรอกซีอะพาไทต์ ต่อการหายของวิการที่กระดูกอัลนาในสุนัข

นางสาว ศศิจรัส ตันตระจักร์

วิทยานิพนธ์นี้เป็นส่วนหนึ่งของการศึกษาตามหลักสูตรปริญญาวิทยาศาสตรมหาบัณฑิต
สาขาวิชาศัลยศาสตร์ทางสัตวแพทย์ ภาควิชาศัลยศาสตร์
คณะสัตวแพทยศาสตร์ จุฬาลงกรณ์มหาวิทยาลัย
ปีการศึกษา 2553

THE EFFECT OF MESENCHYMAL STEM CELLS COMBINED WITH POLYCAPROLACTONE/HYDROXYAPATITE COMPOSITE SCAFFOLD ON THE HEALING OF ULNAR DEFECT IN DOGS

Miss Sasijaras Tantrajak

A Thesis Submitted in Partial Fulfillment of the Requirements
for the Degree of Master of Science Program in Veterinary Surgery
Department of Veterinary Surgery
Faculty of Veterinary Science
Chulalongkorn University
Academic Year 2010

Thesis Title	THE EFFECT OF MESENCHYMAL STEM CELLS COMBINED WITH POLYCAPROLACTONE/HYDROXYAPATITE COMPOSITE SCAFFOLD ON THE HEALING OF ULNAR DEFECT IN DOGS
By	Miss Sasijaras Tantrajak
Field of Study	Veterinary Surgery
Thesis Advisor	Associate Professor Chanin Kalpravidh,D.V.M., M.Sc.
Thesis Co-advisor	Assistant Professor Theerawat Tharasanit,D.V.M., Ph.D.

Accepted by the Veterinary Surgery, Chulalongkorn University in Partial Fulfillment of the Requirements for the Master's Degree

.....Dean of the Faculty of Veterinary Science

(Professor Mongkol Techakumphu, D.V.M., Docterate de 3e cycle)

THESIS COMMITTEE

.....Chairman

(Assistant Professor Voraphan Na Songkhla, D.V.M., Dr. med. vet.)

.....Thesis Advisor

(Associate Professor Chanin Kalpravidh D.V.M., M.Sc.)

.....Thesis Co-advisor

(Assistant Professor Theerawat Tharasanit, D.V.M., Ph.D.)

.....Examiner

(Professor Prasit Pavasant, D.D.S., Ph.D.)

.....Examiner

(Assistant Professor Kumpanart Soontornvipart, D.V.M., Ph.D.)

.....External Examiner

(Niyada Thitaram, D.V.M., Ph.D.)

ศศิจรัส ตันตระจักร์ : ผลของการใช้มีเซนไคมอลสเต็มเซลล์ร่วมกับโครงร่างเซลล์เชิงประกอบระหว่างพอลิคาโพรแลคโตน/ไฮดรอกซีอะพาไทต์ ต่อการหายของวิการที่กระดูกอัลนาในสุนัข (THE EFFECT OF MESENCHYMAL STEM CELLS COMBINED WITH POLYCAPROLACTONE/HYDROXYAPATITE COMPOSITE SCAFFOLD ON THE HEALING OF ULNAR DEFECT IN DOGS)
อ. ที่ปรึกษาวิทยานิพนธ์หลัก: รองศาสตราจารย์ น.สพ. ดร. ชนินทร์ กัลลประวิทธ์,
อ. ที่ปรึกษาวิทยานิพนธ์ร่วม: ผู้ช่วยศาสตราจารย์ น.สพ. ดร. ธีรวัฒน์ ธาราศานิต,
60 หน้า.

วิศวกรรมเนื้อเยื่อกระดูกถือกำเนิดขึ้นเพื่อเป็นอีกทางเลือกหนึ่งในการรักษาความผิดปกติของกระดูกขาบริเวณกว้างโดยอาศัยการการใช้โครงร่างเซลล์ร่วมกับมีเซนไคมอลสเต็มเซลล์ ในการศึกษานี้จัดทำเพื่อศึกษาถึงปฏิกริยาตอบสนองระหว่างมีเซนไคมอลสเต็มเซลล์ของสุนัขและโครงร่างเซลล์เชิงประกอบระหว่างพอลิคาโพรแลคโตน/ไฮดรอกซีอะพาไทต์ จากนั้นทำการศึกษาประสิทธิภาพของโครงร่างเซลล์ชนิดนี้ต่อการหายของวิการที่กระดูกอัลนาในสุนัข ภายหลังการปลูกมีเซนไคมอลสเต็มเซลล์ลงบนโครงร่างเซลล์วันที่หนึ่งพบว่าเซลล์ส่วนมากย้อมติดสีเขียวแสดงถึงการมีชีวิตอยู่ของเซลล์ จากการสังเกตปริมาณเซลล์ที่ติดสีแดปปีร่วมกับการเพิ่มขึ้นของปริมาณโปรตีนอย่างมีนัยสำคัญทางสถิติระหว่างวันที่หนึ่งและห้าและวันที่สามกับห้าตามลำดับ นอกจากนี้เซลล์ที่เกาะอยู่บนโครงร่างเซลล์ยังสามารถเปลี่ยนรูปเป็นเซลล์ออสติโอบลาสต์โดยยืนยันจากการย้อมติดสีอลิซารินเรดในวันที่สิบสี่ของการกระตุ้น ถึงแม้ว่าผลการศึกษาการตอบสนองของมีเซ็นไคมอลสเต็มเซลล์ของสุนัขต่อโครงร่างเซลล์ชนิดนี้ให้ผลเป็นที่น่าพบใจ แต่กลับไม่พบการสร้างกระดูกใหม่ทั้งในกลุ่มที่ได้รับการปลูกฝังโครงร่างเซลล์อย่างเดียวหรือโครงร่างเซลล์ร่วมกับมีเซนไคมอลสเต็ม รอยวิการของทั้งสองกลุ่มพบการสร้างของเนื้อเยื่อพังผืดและหลอดเลือดใหม่อยู่ภายในโครงร่างเซลล์ และเป็นที่น่าแปลกใจอย่างยิ่งในการพบเซลล์ยักษ์ซึ่งมีหลายนิวเคลียสแทรกอยู่ภายในเนื้อเยื่อดังกล่าว แสดงให้เห็นถึงการเกิดปฏิกริยาการอักเสบอย่างเรื้อรังของวิการ

ภาควิชา ศัลยศาสตร์ ลายมือชื่อนิสิต .....
สาขาวิชา ศัลยศาสตร์ทางสัตวแพทย์ ลายมือชื่อ อ.ที่ปรึกษาวิทยานิพนธ์หลัก .....
ปีการศึกษา 2553 ลายมือชื่อ อ.ที่ปรึกษาวิทยานิพนธ์ร่วม .....

5175570231 : MAJOR VETERINARY SURGERY

KEYWORDS : BONE ENGINEERING / MESENCHYMAL STEM CELLS / SCAFFOLD

SASIJARAS TANTRAJAK : THE EFFECT OF MESENCHYMAL STEM CELLS COMBINED WITH POLYCAPROLACTONE/HYDROXYAPATITE COMPOSITE SCAFFOLD ON THE HEALING OF ULNAR DEFECT IN DOGS.

ADVISOR: ASSOCIATE PROFESSOR CHANIN KALPRAVIDH, D.V.M., M.S.,

CO-ADVISOR: ASSISTANT PROFESSOR THEERAWAT THARASANIT, D.V.M., Ph.D., 60 pp.

Bone tissue engineering strategy using biodegradable scaffolds combined with mesenchymal stem cells (MSCs) has emerged as a promising alternative treatment for extensive bone defects. The present *in vitro* study aimed to investigate the interaction between canine MSCs and polycaprolactone/hydroxyapatite (PCL/HA) scaffolds followed by an *in vivo* evaluation of the efficacy of PCL/HA and MSC loaded PCL/HA scaffolds on the healing of canine ulnar defect in dogs.

Viability assay showed that the majority of cells remained viable on day 1 after seeding. An increase in DAPI-stained nuclei density together with a significant increases in total protein concentration ($p<0.05$) was observed between day 1 and 5 and day 3 and 5 after seeding all of which indicated that cells were capable of proliferation over time. Finally, osteogenic differentiation potential of the seeded cells was confirmed by Alizarin staining on day 14 of induction. Despite the promising *in vitro* results, neither new bone nor callus formation was observed in defects treated with PCL/HA alone or MSC-loaded PCL/HA scaffold. Defects in both groups were filled with fibrovascular tissue and remnants of the scaffold. Surprisingly, numerous of multinucleate giant cells were also found within defect sites which strongly

Department : Veterinary Surgery
Field of study : Veterinary Surgery
Academic Year : 2010

Student's Signature Sasijaras T.
Advisor's Signature Chanin Kalpravidh
Co-advisor's Signature Theerawat T.

Acknowledgements

This thesis would not have been possible without the support from many people. First and foremost, I would like to express my sincere gratitude to my advisor Assoc. Prof. Chanin Kalpravidh for his support and encouragement through the study period.

I also would like to express my truthful thank to my co-advisor Asst. Prof. Dr. Theerawat Tharasanit for introducing me into stem cell world and constantly force me to remain focus on my thesis.

I am heartily grateful to all thesis committees (Prof. Dr. Prasit Pavasant, Asst. Prof. Dr. Voraphan Na Songkhla, Asst. Prof. Dr. Kumpanart Soontornvipart, and Instructor Prof. Dr. Niyada Suwankong) for insightful comments and suggestions toward the improvement of this thesis. The gratitude is extended to the Department of Veterinary Surgery and Faculty of Veterinary Science, Chulalongkorn University, 90th years Chulalongkorn Scholarship and Thailand research fund (DBG 5280015) for financial support.

I would like to express my gratitude and appreciation to Prof. Dr. Prasit Pavasant for dedicating his valuable time to help me solving problems with a positive attitude. Asst. Prof. Dr. Kumpanart Soontornvipart, who performed all the surgical procedure in this study, Assoc. Prof. Dr. Wijit Banlunara for histological analysis and interpretation, Instructor Suwicha Chutatep, Miss Nathiwa Chaivoravitsakul and Miss Rumpaipatr Penchome for radiographic analysis and interpretation and Instructor Chalika Wangdee for helping me in the LAB work.

I would like to deeply thank to the Department of Anatomy, Faculty of dentistry for providing PCL/HA scaffold used in this thesis and allow me to use the laboratory facility and the Department of Obstetrics Gynaecology and Reproduction, Faculty of Veterinary science, Chulalongkorn University for shearing the laboratory facility. The gratitude is extended to all of the laboratory dogs that enrolled in this thesis.

Finally, I offer my deepest and heartiest to my beloved family, my father, my mother and my brother for their endless love, patience and constant support. Thank you for always be there whenever I needed.

Contents

List of Tables

List of Figures

CHAPTER I

INTRODUCTION

Importance and Rationale

Extensive bone defect is one of the most common problems in veterinary orthopedics which can be resulted from congenital malformations, traumatic injury, osteomyelitis and bone tumor. Natural bone healing mechanism alone may not be able to regenerate sufficient amount of bone tissue to fill up the large defect consequently result in delayed or nonunion. Therefore, proper surgical intervention and bone healing enhancement are necessary when dealing with such defects (Drosse et al., 2008). There are several approaches to promote new bone formation. Autogenous cancellous bone is considered as the most effective bone graft material because it possesses all four ideal characteristics: osteogenesis, osteoconduction, osteoinduction and osteointegration. In addition, it also has an excellent biocompatibility, elicit no immune response and no risk of disease transmission like allograft (Keating and McQueen, 2001; Griffon, 2005). However, the limited amount of graft available, donor site morbidity and prolonged surgical time are the major drawbacks of autogenous cancellous graft. Therefore, synthetic bone graft substitutes have been introduced as an alternative graft material. Currently, there are various types of synthetic bone graft substitutes which can be categorized into four groups according to the material they are made of biodegradable polymer, ceramic, bioactive glass and their composites. Although there are several types of synthetic bone substitutes, all of them possess only osteoconductive and osteointegrative properties (Moore et al., 2001). Thus new bone formation solely depends on the presence of local osteoprogenitor cells which usually has insufficient number compared to the size of defect (Tabata, 2009). Bone tissue engineering is an emerging field which applies the use of biomaterial scaffolds combined with osteogenic cells creating the biological bone substitutes that have potential for promoting bone regeneration. Among several types of bone scaffolds, biodegradable polycaprolactone (PCL) polymer incorporated with hydroxyapatite (HA)

ceramic composite scaffold has been proposed as a promising candidate for combining with osteopotential cells.

The combination of biomaterial scaffolds and mesenchymal stem cells (MSC) is one of the most promising strategies for bone tissue engineering and cellular delivery (Salgado et al., 2004; Sharma et al., 2005; Necas et al., 2008). Numerous earlier studies suggested that PCL/HA composite scaffolds are good candidates for bone tissue engineering (Azevedo et al., 2003; Ciapetti et al., 2003; Wutticharoenmongkol et al., 2006; Wutticharoenmongkol et al., 2007; Yu et al., 2009). However, most of the successful reports were studied using an *in vitro* model with a lesser extent in small animal models.

Objectives of study

This study aimed to investigate the interaction between canine mesenchymal stem cells and PCL/HA scaffolds with respect to cell viability, adhesion and morphology, proliferative capacity and the ability to differentiate into osteogenic lineage. The second part of the study was performed in order to evaluate the efficacy of PCL/HA alone or PCL/HA combined with canine MSCs on the healing of ulnar critical size defect in dogs. Bone healing was evaluated by serial radiographs every two (2, 4, 6 and 8 weeks postoperation), and histological analysis was performed at 8 weeks after implantation.

Research questions

How do canine MSCs response to PCL/HA scaffold in terms of cell viability, attachment and morphology, proliferative capacity, the ability to differentiate into osteoblastic lineage after seeding onto the scaffold and does defect that implanted with MSC-loaded PCL/HA scaffold showed a superior bone healing in comparison to defect that implanted with PCL/HA scaffold alone or autogenous corticocancellous bone graft.

CHAPTER 2

LITERATURE REVIEW

Natural bone healing

Bone has the unique healing response when facing with injury. Natural bone healing mechanism comprises of three overlapping phases including: inflammatory, reparative and remodeling phase. At the end, the damaged site will be replaced with new bone tissue (Mistry and Mikos, 2005; Krause and Kirker-head, 2006). However, if the injury is severe enough to cause an extensive bone defect, natural healing alone may not be able to sufficiently regenerate a large amount of bone to fulfill the defect. Several approaches have recently been introduced to promote bone healing which requires an understanding of natural bone healing mechanism. The inflammatory phase of bone healing begins immediately after the damage occurred to bone and surrounding soft tissue. Traumatic injury causes disruption of blood vessels inside the marrow cavity which result in hemorrhage to the adjacent tissue and consequently formation of hematoma. Hematoma serves as a primary scaffold for cellular adhesion. In an early stage, platelets, granulocytes, macrophages, lymphocytes and mast cells are the majority of cells that accumulated in the hematoma. These cells are responsible for initiating an acute phase response as a result from releasing of several cytokines and growth factors (Remedios, 1999). The inflammatory response may last for 2-3 weeks following by the recruitment of mesenchymal stem cells (MSCs) and capillary ingrowth. An ingrowth of new vascular tissues provides macrophage and fibroblasts to the damaged site. During the reparative phase, the former hematoma develops into fibrocartilaginous callus bridging over the defect site which eventually be replaced by bone. MSCs play an important role in formation of the callus. Potential sources of MSCs for bone regeneration including endosteum, marrow cavity and cambium layer of periosteum (Ashton et al., 1980). MSCs migrate into the defect site, proliferate and subsequently differentiate into fibroblasts, chondroblast or osteoblast. Level of oxygen tension has major impact on MSCs differentiation. High oxygen tension area such as periosteum, MSCs differentiate directly into osteoblasts result in formation of external

callus (intramembranous ossification). Whereas, MSCs in low oxygen tension area become fibroblasts or chondroblasts, leading to the formation of fibrocartilaginous callus. After new capillaries have invaded, mineralization occurs and the intermediated fibrocartilagenous callus gradually replaces by the woven bone via endochondral ossification (Sfeir et al., 2005). The remodeling phase is the last and longest period of bone healing. In this phase, the new bone tissue undergoes the remodeling process in order to restore the structural and functional properties of the native bone. Osteoclasts begin to resorb the woven bone followed by the formation of the lamellar bone and reorganization of the haversian system. Remodeling of the callus restores the shape and integrity, reestablishing the harversian canal and reformation of the marrow cavity (Samuelson, 2007). As aforementioned, repairing an extensive bone defect requires additional intervention to promote natural bone healing. Several alternative approaches have been conducted to overcome the problems with the use of autogenous cancellous graft. Among the novel bone healing enhancements, bone tissue engineering has been receiving a major attention from researchers over the past decades (Salgado et al., 2004; Porter et al., 2009).

Bone tissue engineering

Langer and Vacanti (1993) originally defined the term “tissue engineering” as an interdisciplinary field which applies the principle of bioengineering, material science and life science toward the development of biological substitutes that restore, maintain and improve tissue function. A combination of cells, scaffolds and growth factors create biological tissue substitutes that have an ability to promote natural tissue healing in the defect sites. There are three principal strategies of tissue engineering: (1) *In situ* tissue regeneration; (2) Implantation of freshly isolated or cultured cells and (3) Implantation of a bioactive substitute assembled *in vitro* from cells and scaffold (Meyer and Wiesmann, 2006). For *in situ* regeneration, new tissue formation is stimulated using scaffolds or external stimuli promoting local progenitor cells at the defect area. The second stategy is to inject individual cells or small cellular aggregates directly to the site with or without scaffold. The problems related with this strategy are the number of cells retained in the injected site is relatively low and cells can hardly accumulate or adhere to the host tissue. (Tabata, 2009) The third strategy, tissue implantation, has been known as one of

the most promising approaches for promoting new bone formation. A three-dimensional biological substitute is engineered in vitro followed by implantation into the defect site. For bone tissue engineering, Bone marrow-derived mesenchymal stem cell combined with biomaterial scaffolds provide the bioactive substitutes that have potentials to enhance bone regeneration, instead of implantation only just non-viable inert materials. (Lui and Ma, 2004; Dickson et al., 2007)

Mesenchymal stem cells

Mesenchymal stem cell (MSC) is one of the adult stem cells which possesses the two remarkable characterizations including the self-renewal capacity and the ability to differentiate along mesenchymal lineage such as osteoblats, chondroblast and adipocyte under an appropriate condition (Pittinger et al., 1999). MSCs reside in various tissues such as bone marrow, adipose tissue, skin, periosteum and placenta (Toma et al., 2001; Tondreau et al., 2004; Miao et al., 2006; Bunnel et al., 2007). Bone marrow is considered as a primary source of MSCs for bone engineering application due to the ease of harvesting and isolating procedure (Tuan et al., 2002). Martin and his colleagues (2002) demonstrated the frequency of feline MSCs in bone marrow mononuclear cell fraction in the range 1 in 4.7 to 5.9 x 10^5 cells which is closely to the frequency of other species (Pittinger, 1999; Wexler et al., 2003). Due to a very small number of MSCs resided in the bone marrow, isolation, cultivation and expansion *ex vivo* are requisite prior seeding them onto the scaffold (Robert et al., 2008).

Scaffold for bone tissue engineering

Scaffold is a three-dimensional porous structure with interconnection between pores which has a capacity to support cell attachment, proliferation and subsequently differentiation into specific cell lineage (Hutmacher et al., 2007). For bone tissue engineering, scaffolds serve as a vehicle for cell delivery and provide initial mechanical support to the defect site. The physical and biological properties of scaffold should resemble to the native extracellular matrix (ECM) in order to optimize new tissue regeneration (Shor et al., 2007). Without the internal porosity and the appropriate pore diameter, new bone formation cannot occur (Kuboki et al., 1998). An ideal bone scaffold should have a high porosity to provide void spaces for stem cell proliferation and then differentiation into osteogenic lineage. Moreover, an interconnecting pore network

facilitates bone tissue formation and vascular ingrowth and transportation of nutrients and metabolic products. Finally the scaffold degradation rate should match with the rate of bone tissue regeneration in order to retain structural integrity until the new bone formation occurs (Cornell, 1999; Martinez and Walker, 1999). The study of Hulbert and his colleague (1970) established the minimal pore size requirement for bone scaffold is 100 μm which relates to the diameter of the haversian system. In addition, scaffolds with the pore sizes larger than 300 μm are favorable to vascular tissue ingrowth which is an important factor for bone regeneration (Karageorgiou and Kaplan, 2005; Mygind et al., 2007). Mygind et al. (2007) compared the effect of pore diameters on human mesenchymal stem cells (hMSCs) using coralline hydroxyapatite scaffolds with two different mean pore sizes 200 and 500 μm. The 200 and 500 μm pore scaffolds have pore diameters between 100-200 and 300-500 μm, respectively. Cell proliferation rate was evaluated by measuring of the amount of extracted DNA from scaffolds and the degree of osteogenic differentiation was assessed by alkaline phosphates activity (ALP activity) combined with the real-time quantitative polymerase chain reaction (qRT-PCR). This study revealed that the 200 μm pore scaffolds provided more suitable environment for hMSCs differentiation while the higher cell numbers were found in the 500 μm pore scaffolds at all time points. The higher rate of differentiation in the 200 μm pore scaffolds may due to the relatively smaller internal spaces making the cells reached their 3D confluence faster than cells in the 500 μm scaffolds consequently an earlier osteoblastic differentiation. Moreover, higher cell density in the 200 μm pore scaffolds enhanced cell to cell interaction via gap junctions which is important for hMSCs differentiation. On the other hand, the 500 μm pore scaffolds exhibited a greater proliferation rate and also a higher number of cells accumulation as shown by DNA quantification test. These may result from the 500 μm scaffolds had bigger pore sizes which facilitated the oxygen and nutrients transportation, provided larger internal space which required more cells to reach 3D confluence. It is notable that direct bone formation occurred without formation of intermediated cartilage when implanted honey-combed-shaped hydroxyapatite scaffolds with the larger tunnel diameter (350 μm). In contrast condrogenesis occurred before osteogensis in the group receiving smaller tunnel diameter scaffold (90-120 μm).

Polycaprolactone scaffold and application

Apart from structural property of scaffolds, the nature of biomaterial also plays an important role in bone regeneration. A wide range of scaffold materials has been investigated for bone tissue engineering including, biodegradable polymers, ceramics and bioactive glasses. PCL is a biodegradable synthetic polymer which has been extensively investigated as a scaffold for bone tissue engineering (Williams et al., 2005; Amato et al., 2007; Guarino et al., 2008; Porter et al., 2009). PCL is a semi-crystalline hydrophobic polymer which belongs to an aliphatic polyester family. PCL offers advantages over others polymeric materials including, good biocompatibility, higher and prolonged mechanical strength, more stable in ambient condition, and slower biodegradation rate which is suitable for bone formation and remodeling phase (Shor et al., 2007; Gunatillake and Adhikari, 2003). The degradation of PCL involves the hydrolytic degradation through de-esterification which can proceed in surface or bulk degradation pathway resulting in the releasing of acidic degradation products, caproic acid. The degradation rate of PCL depends on its molecular weight. The higher molecular weight of PCL, the greater number of ester bonds which requires longer period of degradation (Rezwan et al., 2006). Rohner et al. (2002) studied the effectiveness of PCL, bone marrow coated PCL and poly (lactide-co-DL-lactide) (PLLA/PDLA) on craniofacial defect reconstruction in 10 Yorkshire pigs. A 1.5x2.5 cm critical sized defect was created at the medial wall of both orbits and cast with silicone material for three days then all 20 defects were randomly treated with four different reconstruction techniques and none of the animals had the same technique in both orbits. In group 1, defects in this group were left empty to serve as controls; group 2, defects were reconstructed with 0.5 mm of PLLA/PDLA foils; group 3, defects were reconstructed with PCL scaffolds and group 4, defects were reconstructed with bone marrow coated PCL scaffolds. All pigs were sacrificed three months later and the heads were cut to evaluate the efficacy of the reconstruction techniques. From the histological analysis, neither infection nor inflammation was found in all four groups which represent an excellent biocompatibility of the materials. The defects treated with bone marrow coated PCL scaffolds provided the most promising results as shown by the highest amount of new bone formation compared with other three techniques, all the defects

were completely reconstructed and bone remodeling was found in the middle of the scaffold. The defects that left untreated were covered with fibrous tissue which depressed into the defect site. Little signs of new bone formation were found in the border zone of the defect. Schuckert et al. (2009) previously reported the successful reconstruction of the anterior mandible with PCL scaffold combined with platelet rich plasma (PRP) and recombinant human bone morphogenetic protein-2 (rhBMP-2). The patient was a 71 year old woman, suffered from osteomyelitis of the anterior mandible which caused by bacterial infection of the former titanium implant. The lesion was profound periimplantitis with a significant bone lost. The first intervention was to remove the implant followed by antibiotic and PRP administration. After the defect was closed, the second operation was performed to implant the PCL scaffold soaked with PRP and rhBMP-2. Comparing the radiography and CT scan preoperatively and 4, 6 months postoperatively, new bone formation was ingrowth and filled the defect site. Moreover, an increase in the postoperative average grey value represented more bone density in the implanted site. Several *in vivo* studies have been conducted which demonstrated the promising outcomes of the use of PCL scaffolds for bone tissue engineering application (Rohner et al., 2003; Williams et al., 2005; Oh et al. 2007; Savarino et al., 2007; Dupont et al. 2010).

Despite the fact that biodegradable polymers possess several desirable characteristics for bone tissue regeneration, applications of pure polymeric-based scaffold are limited because of lacking mechanical property, intrinsic hydrophobic chemical nature. Moreover, implantation of large polymeric scaffold may result in massive release of acidic products leading an excessive inflammatory response and consequently formation of a sterile abscess (Böstmann et al. 1990; Bergsma et al., 1995; Prokop et al., 2004). To overcome these limitations, addition of bioceramic into PCL scaffold enhances scaffold characteristics by combining advantages from both materials. Rai et al. (2007) successfully fabricated three-dimensional polycaprolactone-20% tricalcium phosphate (PCL-TCP) scaffolds by fused deposition modeling technique. These scaffolds were tested to investigate the efficacy for promoting the healing of mandibular critical sized defects in dogs. Three rectangular critical-sized defects (18x10x7 mm) were created either in the left or right mandible. On one side of

the mandible, two defects were created at the frontal and caudal part of the mandible while the other defect was created at the caudal region of the other mandible which served as the control group. The defects were randomly treated with PCL-TCP scaffold alone or PCL-TCP scaffold loaded with PRP. To investigate the bone healing, quantitative assessment of bone volume fraction (BVF) by micro-CT analysis was used at 6 and 9 months post implantation. BVF represented the percentage of a volume of interest that was mineralized. Moreover, histological analysis was also carried out in the same sample. From micro-CT evaluation, defects that treated with PCL-TCP scaffolds alone displayed a significant increase in BVF form 5.07 ± 2.13 to 9.78 ± 1.11 at 6 and 9 months, respectively. In PCL-TCP scaffolds loaded with PRP group also showed a significant increase in BVF from 10.1 ± 3.24 to 15.5 ± 1.89 at 6 and 9 months which were higher than BVF of the group that received PCL-TCP scaffold alone in all time points.

Hydroxyapatite (HA) ($Ca_{10}[PO_4]_6[OH]_2$) is known as a ceramic of choice for bone tissue engineering because it has excellent biocompatibility due to the chemical and crystal properties resemblance to the mineral component of bone tissue. Combining HA with PCL PCL-based scaffold helps improve mechanical properties, osteoconductive and osteointegrative potential (Silvio et al., 2002; Wang, 2006; Neuendorf et al., 2008). HA possesses both osteoconductive capacity and ability to bind directly to host bone. In addition, the resorption products of HA help in maintaining local pH by buffering acidic degradation products from PCL degradation (Hutmacher, 2000; Khan et al., 2008; Oh et al., 2006). The PCL/HA composite scaffold possesses more hydrophibic character, increase compressive strength and promoting better cell-scaffold interaction compare with pure PCL. (Calandrelli et al., 2004; Chen and Sun, 2005; Heo et al., 2007; Shor et al., 2007; Fabbri et al., 2010) Wutticharoenmongkol et al. (2006) compared the potential of the electrospun PCL mats and the solution-cast PCL films alone or incorporated with either calcium carbonate ($CaCO_3$) or HA particles. For qualitative comparison, human osteogenic sarcoma cells (SaOS2) were seeded onto these two groups of scaffolds to evaluate the attachment, proliferation and differentiation. The scaffolds were cut into a regtangular shape (10 mm x 70 mm) then seeded with $SaSO_2$ at a density of 36,000 cells/cm^3. Apparently the electrospun PCL mats showed significantly better attachment and proliferation rate in comparison with solution-cast PCL film. In day 3, electrospun

PCL filled with 1.0% w/v HA (FB_HA1.0) exhibit the highest proliferation and alkaline phoaphatase activity compared to those filled with 1.0% $CaCO_3$ and unfilled electrospun mat. Similar positive result was found in the study of Wutticharoenmongkol and group in 2007 using mouse cavaria-derived pre-osteoblastic cells (MC3T3-E1) seeded on to tissue-culture polystyrene plate (TCPS), PCL alone or PCL/HA combined with 1.0% w/v HA fiber mat (PCL/HAp). The PCL/HAp group exhibited the highest amount of new bone formation as shown by osteocalcin (OC) expression and Alizarin Red S staining compared with other two groups. However, the attachment and proliferation of MC3T3-E1 on TCPS were significantly greater than both PCL and PCL/HAp groups. These might result from the hydrophobicity of the material. It is notable that even though PCL had better cell attachment, the greater number of MC3T3-E1 was found on day 3 after cell seeding. Thus the presence of HA particle helps enhance PCL polymer property for bone tissue engineering application. Because of electrospinning technique can produce PCL/HA composite scaffold only in fiber mat form, these scaffolds might not be material of choice for bone tissue engineering as three dimensional structures is one of the fundamental requirements (Sachlos and Czernuszka, 2003). Recently Chuenjitkuntaworn et al. (2010) successfully fabricated PCL/HA scaffolds by solvent casting and particular leaching technique and investigated the characterization and potential application of these scaffolds for bone engineering. For *in vitro* study, primary human alveolar bone cells were used to evaluate the capacity of PCL/HA on cell proliferation and mineralization after seeding onto the scaffolds. MTT results showed the higher number of cells was found within PCL/HA scaffold in comparison with PCL scaffold alone. In addition, primary human bone cells exhibited the greater expression of bone marker proteins (type 1 collagen and osteocalcin) and more calcium deposition as demonstrated by a reverse-transcription polymerase-chain reaction (RT-PCR) and Alizarin Red-S staining. For *in vivo* study, two circular calvarial defects with 4 mm in diameter were created in 6 mice. A total of 12 defects were randomly treated with PCL alone, PCL/HA and the rest were left empty without any treatment. All of the animals were euthanized at 6 weeks after implantation and the calvarial samples were subjected to histological and histomorphometric analysis. The defects treated with PCL/HA exhibited the highest amount of new bone formation compared to those treated with PCL

scaffold alone while fibrous tissue with minimal mineralization was found in the defect site that left empty.

From the promising outcomes of the used of PCL/HA composite scaffolds as aforementioned, we hypothesized that these composite scaffolds may have similar ability for treatment a large bony defect in dog. This study was carried out to investigate the interaction between canine mesenchymal stem cells and the PCL/HA scaffolds with regard to cell viability, attachment and morphology, proliferative capacity, the ability to differentiate into osteoblastic lineage after seeding and subsequently the efficacy on healing ulnar critical sized defect in dogs. Bone healing was evaluated by radiographic and histological analysis.

CHAPTER 3

MATERIALS AND METHODS

Scaffolds

PCL/HA composites scaffolds used in this study were kindly provided by Faculty of Dentistry, Chulalongkorn university. Scaffolds were from Polycaprolactone (PCL; Aldrich, USA; *M*w = 80,000 $g \cdot mol^{-1}$) incorporated with 40% w/w HA powder by solvent casting and particular leaching technique. Sucrose with diameter around 400–500 μm was used as the porogen to create the interconnected network. The scaffold porosity was in the range of 85-87%.

Animal

All protocols used in this study were approved by the Committee for the Ethical Care of Animals of the Chulalongkorn University. Seven mongrel dogs were enrolled in this study with various sexes (male=2, female=5), body weights were ranging from 12 to 16 kg. In each dog, a 2.5 cm bilateral ulnar ostectomy was performed to create critical sized defects. One dog had to undergo the second operation in order to get the total of 15 defect sites. Complete blood counts and blood chemical profiles were also examined prior surgery. All efforts were made to minimize animal suffering, pain and the number of animal used.

Anesthetic protocols

Dogs were withheld water and food for 12 hours before surgery and allowed to urinate and defecate before anesthesia. Routine physical examination and physiological parameters including body temperature, heart rate, respiratory rate, mucous membrane color, capillary refilled time and hydration status were measured prior the premedication to use as baseline data for the anesthetic monitoring.

Acepromazine maleate (0.02 mg/kg) (Vetranquil™, Ceva Sante animal, Libourne, France) combined with morphine sulphate (0.5 mg/kg) (Food and drug administration, Bangkok, Thailand) were used as the premedication drugs which administered intramuscularly. General anesthesia was induced with 4-6 mg/kg propofol (Fresenius Kabi Austria GmbH, Graz, Austria) intravenously. During operation, an anesthetic level

was maintained by an inhalation anesthesia using isoflurane in 100% oxygen via the rebreathing anesthetic circuit. The concentration of isoflurane was adjusted to maintain the surgical plane of anesthesia according to the eye position, palpebral reflex, jaw tone and lack of response to noxious stimuli. All dogs received crystalloid solution intravenously at the rate of 5-10 ml/kg/h during operation. Cefazolin (250 mg/ml) 25 mg/kg was administered intravenously as the prophylactic antibiotic.

A. Epidural anesthesia

Epidural anesthesia was performed in order to relief pain sensation caused by bone marrow aspiration procedure. Dog was positioned in sternal recumbency with both hindlimbs extended cranially and parallel to the body. The lumbosacral space was located by using the bony prominence of both wings of ilium and dorsal spinous process of the 7^{th} lumbar vertebrae as the landmark. An epidural needle was inserted into the epidural space and slowly administered an epidural drug containing 0.5% bupivacaine 1 mg/kg combined with morphine 0.1 mg/kg (Skarda and Tranquilli, 2007).

B. Brachial plexus block

Brachial plexus block helps to minimize pain sensation by inhibiting noxious signal before enter to the spinal cord by using 0.5% bupivacaine 1.3 mg/kg prior bilateral ulnar ostectomy 30 minutes. Dog was positioned in lateral recumbency, the shoulder area was prepared by aseptic technique. A 7.5 cm, 22 gauge spinal needle was inserted through the medial side of the shoulder joint in a direction parallel to the vertebrae, gently advanced until the tip of the needle seated close to the brachial plexus and connected the end of the needle with a syringe containing 0.5% bupivacaine and drawback to make sure that the needle was not placed in blood vessel. Administer approximately two-third of the total volume of bupivacaine and then injected the remaining volume while the needle was slowly withdrawing.

Bone marrow aspiration

Four of the seven dogs were randomly selected to collect bone marrow samples for further MSCs isolation, characterization and subsequently seeding onto the scaffolds. Dog was positioned in lateral recumbency. Small skin and subcutaneous tissue was incised above the dorsal iliac crest of the ilium. A bone tunnel was created by using 2.5 mm pin followed by insertion of a 16G, 1 inch long Rosenthal needle through

the guide hole. Once the needle was placed into the marrow cavity, a 5 ml syringe containing 1 ml of heparin (100 IU/ml) was connected to the needle. In each dog, the total volume of the aspirated bone marrow was 10 ml. The subcutaneous tissue and skin were closed in a simple interrupted pattern using polydioxanone 3-0 (PDS II; Ethicon, USA) and polyamide 3-0 (Ethilon; Ethicon, USA), respectively.

MSCs isolation and culture expansion

In an attempt to enhance MSCs in the initial cell population, 5 ml of red blood cell lysing buffer (8.3 g/L ammonium chloride in 0.01 M Tris-HCl buffer pH 7.5 $\pm$ 0.2; Sigma-Aldrich, USA) was added into 5 ml aspirated bone marrow in a 15 ml sterile plastic tube (BD Falcon™, Becton Dickinson, Thailand). The solution was gently mixed followed by centrifugation at 1000 rpm for 5 minutes at 26 $^{\circ}$ C. The supernatant was discarded and the pellet was resuspended with red blood cell lysing buffer in a 1:1 ratio. The mixture was recentrifuged in the same condition but this time the pellet was resuspended with 1 ml of MSC culture medium containing low-glucose Dulbecco's modified Eagle's medium (low glucose DMEM; Sigma, USA.) supplemented with 10% (v/v) fetal bovine serum (FBS) (Invitrogen, Carlsbad, USA), 2 mM L-glutamine, 100 unit/ml penicillin G, 100 µg/ml streptomycin and 5 µg/ml amphotericin B. Cells were plated in 100 mm tissue culture dish (BD Falcon™, Thailand) in 6 ml of culture medium. The initial seeding density was approximately between 50-60% confluences. The culture plate was gently mixed before incubated at 37°C in 5% humidified CO_2.

During the culture period, the cultured cells were rinsed with Dulbecco's Phosphate-Buffered Saline (DPBS, Invitrogen) to remove the non-adherent cells and the culture medium was replaced every 1-2 days. Subculture was performed once the cell reached approximately 80-90% confluence. After the culture medium was removed, MSCs were dissociated using 0.05% trypsin-EDTA (Gibco, Invitrogen). The enzyme was inactivated by adding 4 ml of 10% fetal bovine serum in DMEM. Cell suspension was pipetted into a 15 ml tube and centrifuged at 1000 rpm at 4 $^{\circ}$C for 5 minutes, then the supernatant was discarded and pellet was resuspended with 1 ml of MSC culture medium.

MSCs characterization

The isolated MSCs of 1 from 4 dogs were randomly selected to characterize the MSCs population as the following procedures.

A. The ability to adhere to plastic surface

Plastic adherence is a well-known physical property of MSCs which can be used as an isolation technique. Cell morphology and the ability to adhere to plastic surface were observed by using a phase contrast microscope (CKX41; Olympus, Shinjuku, Japan). Trypan dye exclusion test was conducted on the seventh day of culture in order to evaluate the cell number and viability. Briefly, cells were trypsinized and stained with trypan blue in 1:1 ratio. The total adherent cells number was counted using a hemocytometer. The total number of adherent cells and the viable percentage were calculated.

B. Expression of cell-surface antigen markers

Flow cytometry was performed in order to determine the expression of surface antigen of canine MSCs. Canine MSCs at passage 3 were trypsinized and resuspended with stained medium (1% FBS in PBS). The cell suspension was divided into 20,00-30,000 cells to stained with Rat monoclonal anti-canine CD 34 conjugated with Fluorescein isothiocyanate (FITC) which served as negative marker for MSC. Two MSCs positive markers: rat monoclonal anti-canine CD 90 (AbD serotec, Kidlington, UK) with Rabbit anti-rat FITC secondary antibody and monoclonal anti-canine CD44 conjugated with Allophycocyanin (APC) (R&D system, Minneapolis, USA) were used in this study. MSCs labeling protocol was followed the manufacturer's recommendations. The fluorescent MSCs were fixed with 1% paraformaldehyde and kept at 4ºC. Unstained MSCs and MSCs stained with secondary antibody alone were used as controls.

C. The potential to differentiate into mesenchymal lineages

Canine MSCs at passage 3 were used to evaluate the capacity of multilineage differentiation. Before the induction, cells were raised in normal MSC culture medium. Once the confluence reached 70-80%, the specific condition was introduced regarding to the particular cell line as illustrated in table 1 (Bosch et al., 2006). Histochemical special stains were carried out in order to validate the differentiation capacity of canine MSCs on the 21 day of induction as described in table 2.

a. Osteogenic differentiation was induced when MSCs reached 80% confluence. MSCs were treated with bone induction medium which composed of low glucose DMEM supplemented with 10% (v/v) FCS, 0.1 µM dexamethasone, 50 µg/ml ascorbic acid and 10 mM beta glycerophosphate. The culture cells were fixed with 10% paraformaldehyde and stained with Von Kossa and Alizarin Red to confirm osteoblastic differentiation.

b. Two types of specific media, namely adipogenic induction and adipogenic maintenance medium were required for adipogenic differentiation. An Adipogenic induction medium was comprised of low glucose DMEM supplemented with 10% (v/v) FCS, 0.1 mg/ml human recombinant insulin, 10 mM sodium pyruvate, 1 mM methyl isobutylxanthine (IBMX), 0.2 mM indomethacin and 1 µM dexamethasone. For Adipogenic maintenance medium, the medium was prepared in the same manner as Adipogenic induction medium but excluding IBMX, indomethacin and dexamethasone. The culture cell was stained with Oil Red O to confirm the adipogenic diferrentiation.

c. Two essential conditions for chondrogenic differentiation were a three-dimensional culturing pattern by gently centrifuged cell suspension into a pellet and a special medium for chondrogenic induction containing 0.1 µg/ml TGF-ß1, 0.1 µM dexamethasone and 50 ng/ml acorbic acid 2-phosphate in low glucose DMEM without the presence of FBS. Alcian blue dye was used to confirmed the chondrogenic differentiation.

Table 1 specific stimulus for inducing MSCs differentiation into mesenchymal lineage (Bosch et al., 2006)

Lineage	Differentiation medium
Osteogenic	0.1 µM dexamethasone, 50 µM ascorbic acid and 10 mM ß-glycerol phosphate
Adipogenic	1 mM IBMX, 0.1 mg/ml human recombinant insulin, 0.2 mM indomethacin and 1 µM dexamethasone
Chondrogenic	10 ng/ml TGF-ß1, 0.1 µM dexamethasone, and 50 ng/ml acorbic acid 2-phosphate

Table 2 The histochemical special staining for evaluating MSCs differentiations

Cell types	Special staining
Bone	Von Kossa
Adipose tissue	Oil Red O
Cartilage	Alcian blue

Cell and Scaffold preparation

PCL/HA composite scaffolds were cut into 5 x 5 x 5 mm and 10 x 5 x 25 mm for *in vitro* and *in vivo* studies, respectively. The scaffolds were sterilized with 100% v/v absolute ethanol for 1 hour and washed thoroughly with steriled distilled water and DPBS to remove residual ethanol. The scaffolds were preconditioned in culture medium for 2 hours prior to seeding procedure.

For *in vitro* study of cell/scaffold interaction, PCL/HA scaffolds were seeded with canine MSCs at a density of 100,000 cells/scaffold and for *in vivo* study, MSCs approximately 20 x10^6cells/ml was used. The loaded scaffolds were incubated at 37° C in 5% humidified CO_2. After 45 minutes of incubation, 5 ml of culture medium was added to cover the entire implant.

MSC morphology and adhesive characterization

Scanning electron microscope (SEM) was performed to illustrate MSC morphology and the ability to attach on the PCL/HA scaffold on day 1, 3 and 5 after seeding. Briefly, the loaded PCL/HA scaffolds were washed twice with PBS (pH 7.2) and fixed with cold 3% glutaraldehyde for 30 min. Then, the scaffolds were dehydrated with serial ethanol dilution (30%, 50%, 70%, 90% and 100% (v/v) ethanol, respectively) for 2 min at each concentration. Finally, the scaffolds were soaked with Hexamethyldisilazane (HMDS) for 5 min and allow to dry overnight at room temperature, so that HMDS was evaporated from the scaffolds before coating with gold and examining under JSM-5410LV scanning electron microscopy (JEOL, Japan).

MSC viability, proliferative capacity

After 1 day of seeding, MSC-loaded scaffold was fixed with 3.7% paraformaldehyde and cut into thin sections for evaluation of canine MSC viability by dual fluorescent staining method using calcein AM and ethidium homodimer. A bright green fluorescence from calcein AM demonstrated viability of MSC while dead cell exhibited red fluorescent color. For MSC proliferation evaluation, PCL/HA scaffolds were seeded with canine at a density of 50,000 cells/scaffold. The proliferative capacity was qualitatively analyzed based on the serial fluorescent images of canine MSCs staining with 4', 6-diamidino-2-phenylindole dihydrochloride (DAPI; Roche, Germany) in conjunction with a quantitative analysis of the total protein content by the bicinchoninic acid (BCA) protein assay kit (Pierce Biotechnology, USA). For DAPI fluorescence staining, the loaded PCL/HA scaffolds were fixed at day 1, 2 and 4 of incubation with 3.7% formaldehyde. MSC loaded-PCL/HA scaffold were then stained with DAPI (1:1000) for 10 min and observed under Zeiss Axio Observer fluorescence microscope (Carl Zeiss, Germany) at a wavelength of 380 nm. The total protein quantification of MSC-loaded PCL/HA construct was determined on day 1, 3 and 5 after seeding. The BCA assay is a colorimetric detection and quantification of total protein in the cell/scaffold construct by measuring the purple water-soluble product resulting from the chelation of BCA and Cu^{+1}. Briefly, the working solution was prepared by mixing Reagent A and reagent B in the ratio of 50:1. Then the loaded PCL/HA scaffolds were washed twice with PBS to eliminate the contaminated protein from the culture medium and chopped with a shaped scissors into small pieces before adding 200 µl of 2% sodium dodecly sulfate in a 1 ml of microcentrifuge tube. Mixed thoroughly by vortexing for 1 min and centrifuged at 5000 rpm for 1 min. A 50 µm of the supernatant was transferred into new 1 ml of microcentrifuge tube then added 1 ml of working solution, mixed thoroughly by vortexing, and incubated in 37ºC for 30 min. Finally, 80 µl of the final solution was pipetted into a 24-well plate and measured the absorbance at 562 nm wavelength using an absorbance microplate reader (ELx800™; Biotek, Vermont). All data were collected and analyzed by microplate data collection and analysis Software (Gen5™; Biotek, Vermont) with the reference to bovine serum albumin.

Osteogenic differentiation of MSC within PCL/HA scaffold

The ability of canine MSCs to differentiate into an osteoblastic lineage on PCL/HA scaffold was investigated by seeding MSCs at a density of 50,000 cells onto the PCL/HA scaffold size 5 x 5 x 5 mm. The MSC loaded PCL/HA scaffold treated with the bone induction medium on day 3 of culture, and differentiation was confirmed by using Alizarin Red staining on day 14 of induction.

Evaluation of the efficacy of PCL/HA and MSCs on healing of ulnar critical size defects

A. Surgical procedure

To perform bilateral ulnar ostectomy, dogs were anaesthetized as mentioned above. The surgical site was clipped and prepared following the standard aseptic technique. A 10 cm incision was made through the skin and subcutaneous tissue over the caudolateral aspect of the ulna. The incision began approximately 3-5 cm distal to the elbow joint and continue distally along the ulnar shaft. Brachial fascia was incised parallel to the same line then retracted the ulnaris lateralis and flexor carpi ulnaris muscle with the periosteal elevator to expose the ulna. The osteotomized site was marked, and the bilateral 2.5 cm ulnar ostectomy was performed using an oscillating saw. No internal fixation was used in this study due to the canine model is mechanically stability without further fixation as the radius is the major load-bearing structure in the canine forelimb. The fascia and subcutaneous tissue were closed in a simple continuous pattern using polydioxanone 3-0 and skin was closed in simple interrupted pattern using polyamide 3-0. Then, the ostectomy was performed on the contralateral ulna as described above. This provided a total of 15 ulnar critical size defects. In this study, defects on the left ulnae were implanted with the corticocancellous autografts to serve as a control group (group 1, n=7) while defects on the right ulnae were randomly implanted with PCL/HA composite scaffold alone (group 2, n=4) or PCL/HA combined with canine MSCs (group 3, n=4) (table 3). After the operation, all forelimbs were applied with modified Robert Jone bandages reinforced with thermoplastic splints (Vet-lite, BEC, Thailand) for 2 weeks and dogs were received 5 mg/kg enrofloxacin (Baytril; Bayer, USA) and 4 mg/kg carprofen (Rimadly; Pfizer, USA) orally twice a day for 7 days after implantation.

B. Bone healing evaluation

Radiographic evaluation

The craniocaudal (CrCd) radiographs were taken immediately after operation and at 2, 4, 6, 8 weeks postoperatively. Bone healing was evaluated and scored by 3 radiologists in a blinded fashion using the radiographic scoring system described by Jones et al. (2008) (Table 4)

Histological evaluation

At the 8 weeks after implantation. Bilateral ulnar ostectomy was performed again in order to obtain the ulnar specimen. The specimen must be included the middle portion of the implant and the host bone-implant interface. The sample was fixed in 10% buffered formalin, dehydrated and embedded in the paraffin blocks. Finally the sample was cut in the sagittal plane and stained with hematoxylin and eosin (H&E).

Table 3 Groups, number of defects per group and type of implant

Groups	Number of defects	Type of implant
Group 1	7	Corticocancellous graft
Group 2	4	PCL/HA alone
Group 3	4	MSC-loaded PCL/HA

Table 4 Radiographic scoring system for bone healing evaluation (Jones et al., 2008)

Description	Radiographic score
No change from immediate postoperative appearance	0
A slight increase in radiodensity distinguishable from the graft	1
Recognizable increase in radiodensity, bridging of one cortex with new bone formation to the graft	2
Bridging of at least one cortex with material of nonuniform radiodensity, early incorporation of the graft suggested by obscurity of graft borders	3
Defect bridged on both medial and lateral sides with bone of uniform radiodensity, cut ends of the cortex still visible, graft and new bone not easy to differentiate	4
Same as grade 3, with at least one of four cortices obscured by new bone	5
Defect bridged by uniform new bone, cut ends of cortex no longer distinguishable, graft no longer visible	6

Statistical analysis

For total protein concentrations, Leven test was used to assess the homogeneity of variance among the groups and all data were analyzed using analysis of Variance (ANOVA) to determine the difference in protein concentration between day 1, 3 and 5 after seeding. Significance was defined as a p value less than or equal to 0.05.

For radiographic scores which were nonparametric data, Kruskal-Wallis one-way analysis of variance was used to determined the difference in healing efficacy of the implants at 2, 4, 6 and 8 weeks postoperatively. Significance was defined as a p value less than or equal to 0.05.

CHAPTER 4

RESULT

Canine MSCs isolation, cultivation and expansion

Bone marrow was aspirated from the dorsal iliac crest of 4 dogs (Figure 1). To obtained canine MSCs, the aspirated bone marrow contents underwent MSCs enrichment, isolation, culture and expansion. At 24 hours after plating, adherent cells demonstrated heterogeneous morphology including a fibroblastic-like cell, polygonal cell and round cell. Non-adherent cells were removed by changing the culture medium and cells were distributed more homogeneous population of spindle-shaped cells was mainly observed (Figure 2). On the 7^{th} day of culture, trypan dye exclusion test was performed to assess total number of adherent cell and viability percentage. Trypan blue is a tetrasulfonated dye which has been commonly used to distinguish between dead and viable cells because the dye can penetrate only damaged cell wall. The total number of adherent cells on day 7 of culture was 1.327×10^6 cells and the percentages viability was 98.64.

Figure 1 Bone marrow aspiration from the dorsal iliac crest of dog

Figure 2 Canine bone marrow derived mesenchymal stem cells at passage 1 on day 3 of culture (100 X magnification, 500 µm scale bar)

Expression of cell-surface antigen markers

Flow cytometric immunophenotypic analysis of cell surface antigen expression was performed by using CD 34 as a negative marker and CD 44 and CD 90 as positive marker for MSCs while unstained cells and MSCs stained with secondary antibody alone were used as controls (Figure 3). A total of 200,000 to 300,000 cells were stained with each antibody. MSCs at passage 3 were strongly positive for CD 44 and CD 90 whereas the expressions of CD 34 were nearly absent. The percentage of cells positive for each CD was demonstrated in table 5. The percentage of CD 44 expressed by canine MSCs at passage 3 was more than 97% while the percentage of CD 90-positive cells was more than 93%. In addition, less than 1% of MSC population expressed CD 34.

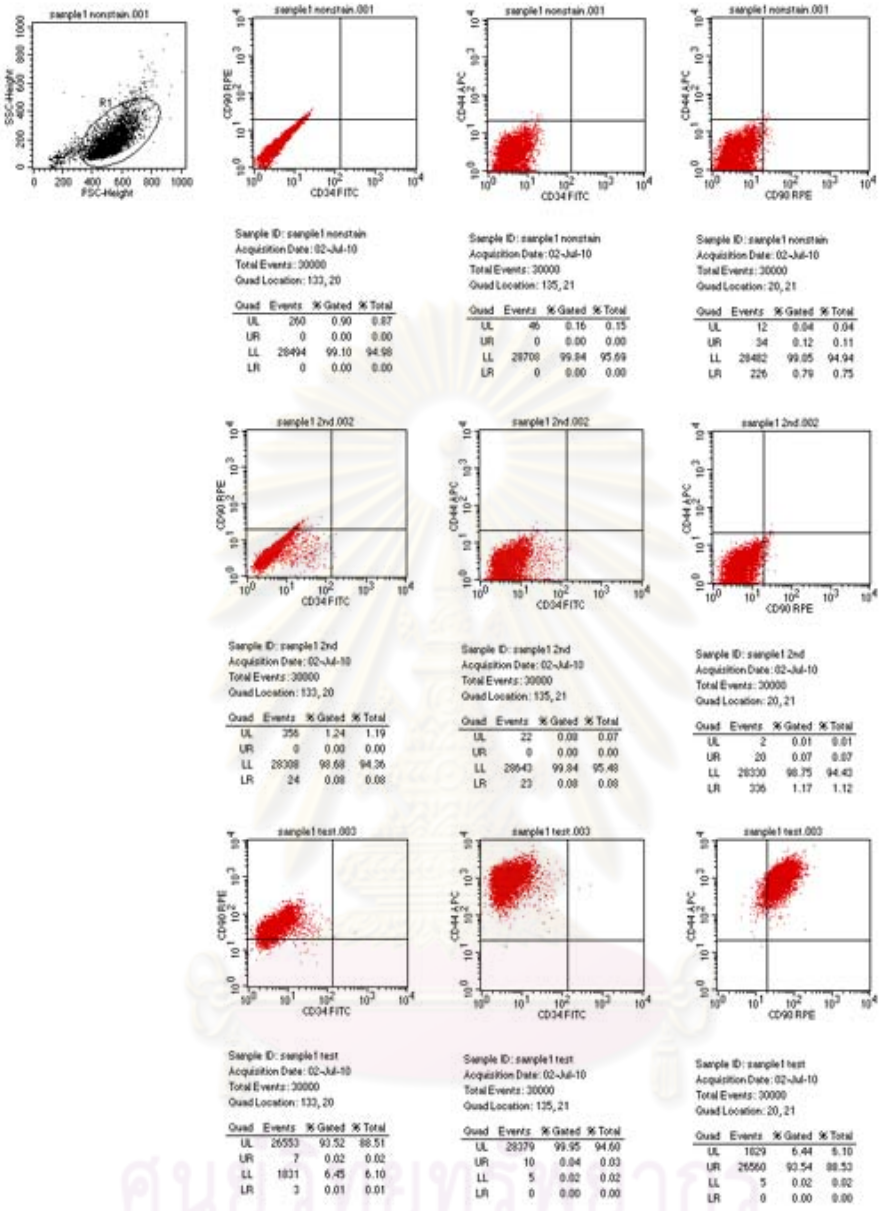

Figure 3 Example of flow cytometric analysis of MSCs surface antigen at passage 3

Canine MSCs differentiation

Canine MSCs at passage 3 were subjected to demonstrate the mesenchymal differentiation capacity with the specific condition according to the cell type. Histochemical special staining was performed in order to verify each differentiation on day 21 after induction. Von Kossa, Oil Red O and Alcian blue staining were used to confirm osteoblastic, adipogenic and chondrogenic differentiation, respectively. Under an osteogenic condition (Figure 4), the former spindle-shaped cells gradually transformed into polygonal, cuboidal, osteoblast-like cells extending their long processes connecting to each other to form a cellular network and started to synthesize the extracellular matrix that was positive to Von Kossa (Figure 5A) and Alizarin Red (Figure 5B). For adipogenic differentiation, thin fibroblastic cells became oval to round-shaped cells with large cytoplasm containing lipid vacuoles stained positively with Oil Red O (Figure 6). Finally, chondrogenic differentiation was achieved by culturing canine MSCs in a pellet cultural system combining with a special chondrogenic induction medium. MSCs were slowly aggregated and developed into a small round nodule within the first week of induction. The nodule was positively stained with Alcian blue indicated the presence of glycosaminoglycans at 3 weeks of induction (Figure 7).

Table 5 The percentage of canine MSCs positive for CD 44, CD 90 and CD 34 determined by flow cytometry at passage 3

		Markers		
Dog	Passage	CD34	CD44	CD90
Dog 1	3	0	99.82	99.21
Dog 2	3	0	99.89	98.02
Dog 3	3	0	99.95	93.52
Dog 4	3	0.06	97.91	96.92

Figure 4 Canine mesenchymal stem cells after osteogenic induction examed under phase contrast microscope (100 X magnification, 500 µm scale bar)

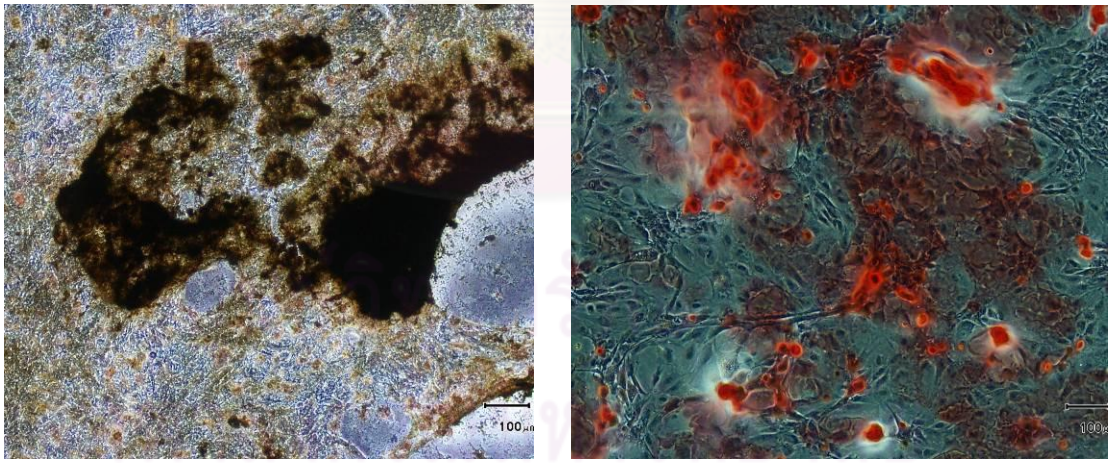

A B

Figure 5 Von Kossa (A) and Alizarin Red (B) staining were used to validate the differentiation capacity of canine MSC into the osteogenic lineage

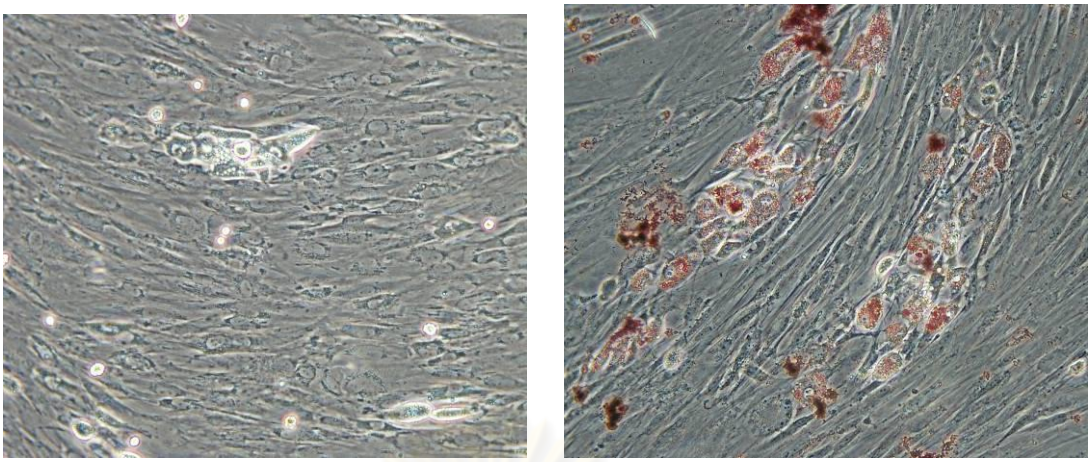

A B

Figure 6 The morphology of canine MSCs after adipogenic induction (A) Confirmation of the differentiation capacity of canine MSC into the adipogenic lineage using Oil Red O staining (B)

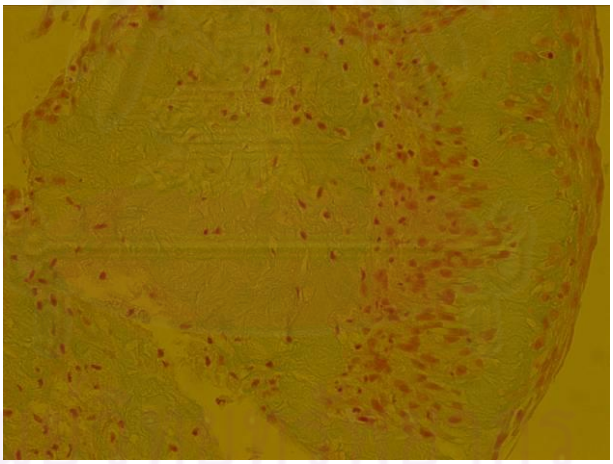

Figure 7 Alcian blue staining was used to validate the differentiation capacity of canine MSC into the chondrogenic lineage

Canine MSCs behavior within PCL/HA scaffold

In vitro studies of canine MSCs behavior on PCL/HA composite scaffold was evaluated in terms of MSC attachment, morphology, the ability to growth and proliferation within the scaffold.

A. MSC viability

The combination of calcein AM and ethidium homodimer fluorescence staining was used to assess MSC viability. A green fluorescence from calcein AM represented the viable MSCs while a red fluorescence indicated the non-viable cells (Figure 8). On day 1 after seeding, a mixed population of viable and non-viable canine MSCs was observed. The majority of the cells exhibited green calcein fluorescence with a small number of cells was labeled with red fluorescence. In addition, MSCs were found throughout the sample represented a good cell distribution within the scaffold.

Figure 8 Fluorescent microscopic finding of canine MSCs viability within PCL/HA scaffold 12 hours after seeding.

B. MSC morphology and adhesive characterization

Canine MSC attachment and morphology was observed by SEM on day 1, 3 and 5 after seeding. On day 1 after seeding, MSCs appeared as flat cells spreading onto the surface of scaffold with finger-like projection of cell membrane (filopodia) adhered to the scaffold (Fig 9A). MSCs became more spread and elongated with an enlargement of adhesive areas between cells and scaffold on day 3 of seeding. In addition, on day 3, more cells were observed and appeared to form small cell clusters with an intercellular connection (Fig 9B).

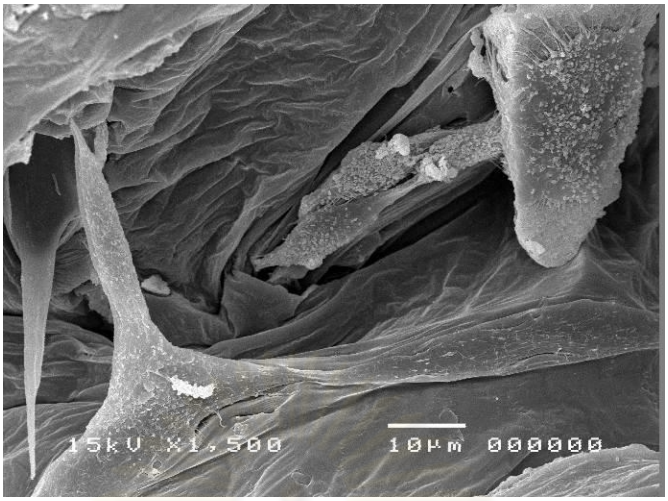

A

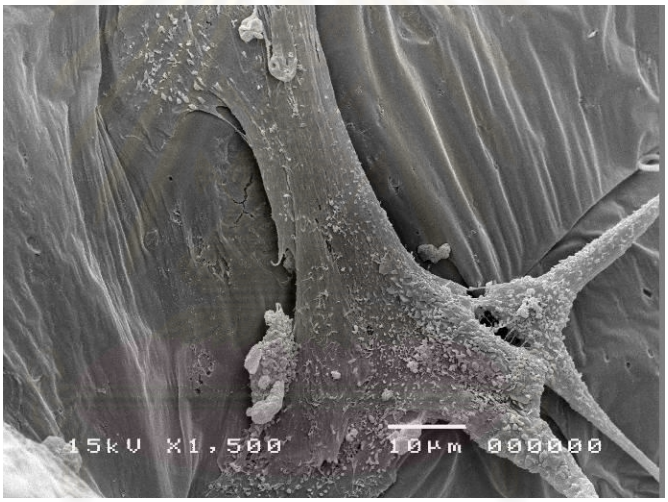

B

Figure 9 Scanning electron microscopic images (1500X magnification and 10 µm scale bar) of canine MSCs attachment and morphology on day1 (A) and 3 (B) of seeding

C. MSC proliferative capacity

The proliferation of canine MSCs within PCL/HA scaffold was determined by qualitative comparison of serial DAPI fluorescent images on day1 (Figure 10A and B), 2 (Figure 10C and D) and 4 (Figure 10 E and F) after seeding. An increase MSC population was observed by an increase in DAPI-stained nuclei density over time. The quantitative analysis of the protein content was conducted to evaluate MSC growth and proliferation within PCL/HA scaffold using the BCA protein assay. The amount of protein (µg/ml) in each samples were calculated from the absorbance of the sample solution measured at a wavelength of 562 nm with reference to the standard protein (Table 6). The total protein concentration of MSC-loaded PCL/HA scaffold on day 1, 3 and 5 was 523±15.27, 626.67±71.12 and 861.67±127.16 µg/ml, respectively. A significant differences were found between protein content of PCL/HA alone and MSC-loaded PCL/HA scaffold at all time points. A significant increase in total protein concentration of MSC-loaded PCL/HA scaffold were observed between day 1 and day 5 and day 3 and day 5 ($p<0.05$). However, no significant difference was found between day 1 and 3 (Figure 11). Notably, the color of the sample solution was changed from green to purple in the proportion to the protein concentration in the scaffold (Figure 12).

D. Osteogenic differentiation of canine MSCs on PCL/HA scaffold

To confirm an osteogenic differentiation potential of canine MSCs after seeding on PCL/HA scaffold, Alizarin Red staining was performed on day 14 of induction. Positive Alizarin Red staining was observed in both PCL/HA scaffolds alone and MSC-loaded PCL/HA scaffolds. After washed the samples several time with PBS, only PCL/HA scaffolds that combined with canine MSCs were still remained positive to Alizarin Red suggested the presence of calcium deposition within scaffolds.

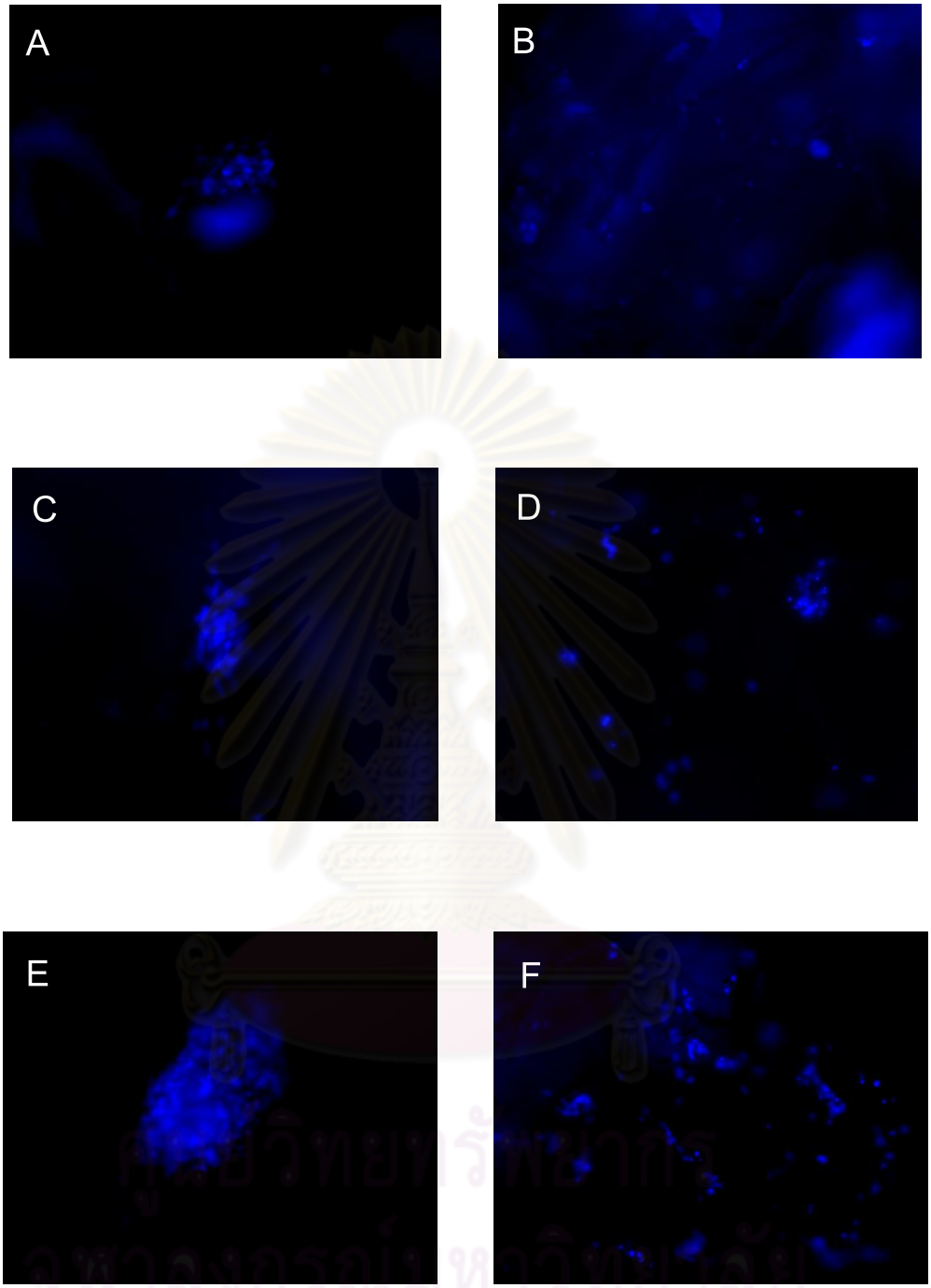

Figure 10 Qualitative visual fluorescence analysis of canine MSC proliferation using DAPI nuclear staining on day 1 (A and B), 2 (C and D) and 4 (E and F) of seeding

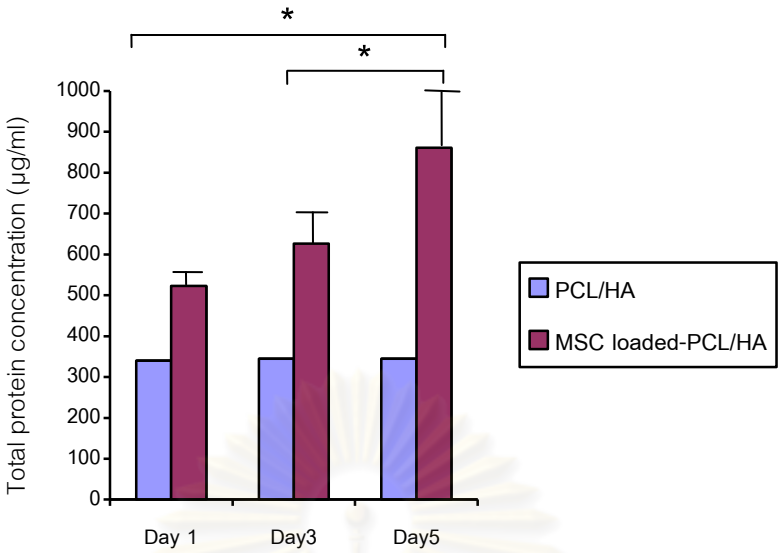

Figure 11 Quantitative measurement of total protein concentrations of PCL/HA and MSC loaded-PCL/HA scaffolds on day 1, 3 and 5 of culture. *Significant increase in protein concentration was observed ($p<0.05$)

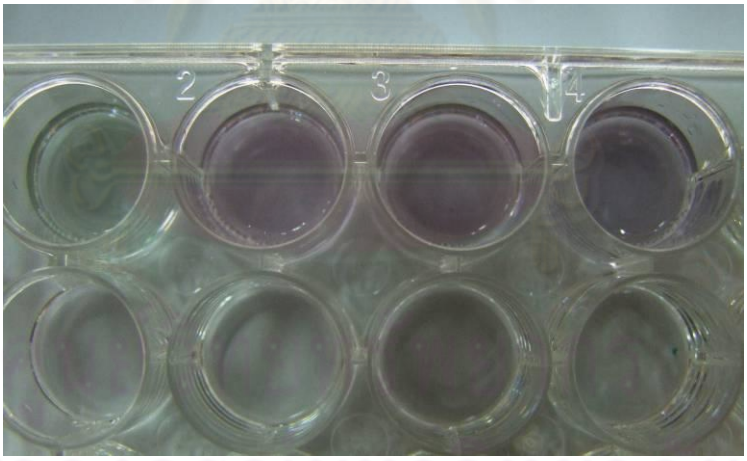

Figure 12 The BCA protein assay. The degree of color change from green to purple is proportional to protein concentration present within the scaffold

Radiographic evaluation

The craniocaudal radiographs of the defects were taken immediately and at 2, 4, 6 and 8 week postoperatively (Fig. 13A, B, C and D) illustrated the progressive bone healing of the ulnar defect that treated with corticocancellous bone graft (group 1). Slightly new bone formation was visible during the first 4 weeks postoperatively. At 6week, the bone bridge formation between graft and host bone was evident at the distal part of the defect. By 8 weeks postoperatively, the bone bridging was clearly observed on both side of cortices. An increase in radiodensity of the graft-host bone interfaces with time demonstrated a progressive healing of the defect. Neither new bone nor callus formation was observed in the defect site treated with PCL/HA alone (group 2) (Figure 14A, B, C and D) and MSC-loaded PCL/HA (group 3) (Figure 15A, B, C and D) at any time point. A slightly increase in radiodensity was observed within the implant site in both groups. There were statistically significant differences ($p<0.05$) in radiographic score between group 1, 2 and 3 at 6 weeks and between group 1 and 2 and group 1 and 3 at 8 weeks postoperatively. No significant differences in radiographic score were detected between treatment groups at 2 and 4 weeks postoperatively ($p>0.05$)

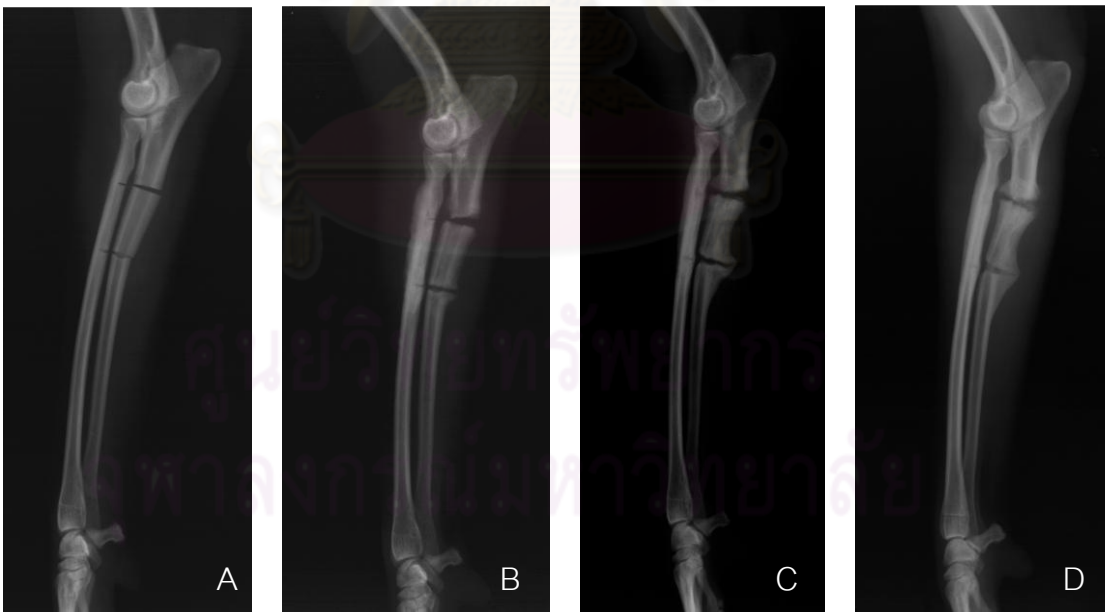

Figure 13 Radiographs of canine ulnar segmental defects treated with the autogenous cancellous bone graft at (A) 2 weeks; (B) 4 weeks; (C) 6 weeks and (D) 8 weeks postoperatively

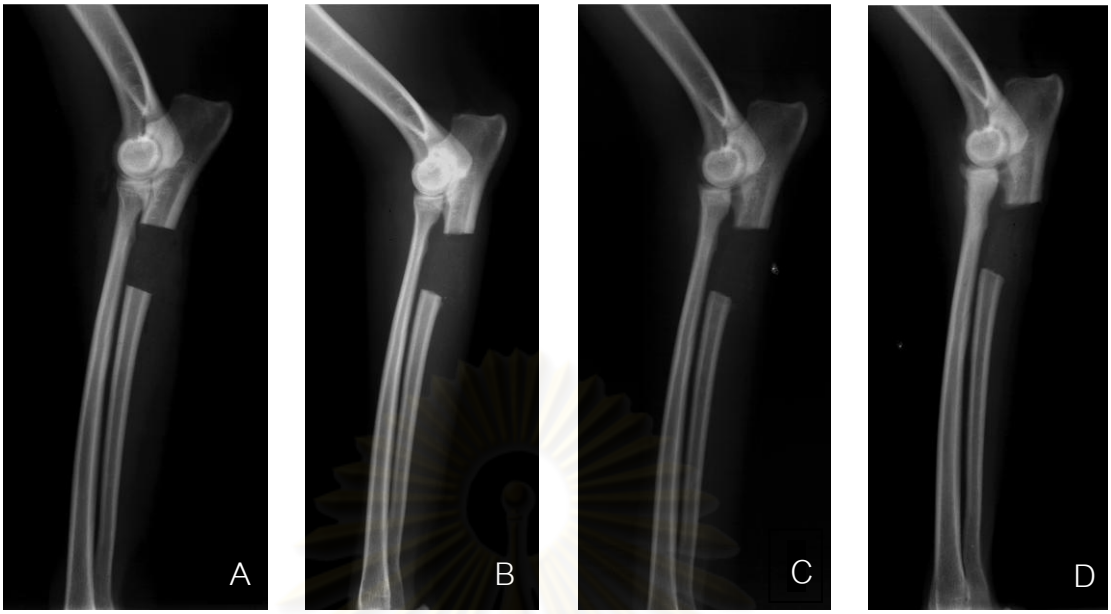

Figure 14 Radiographic images of canine ulnar segmental defects treated PCL/HA scaffold at (A) 2 weeks; (B) 4 weeks; (C) 6 weeks and (D) 8 weeks postoperatively

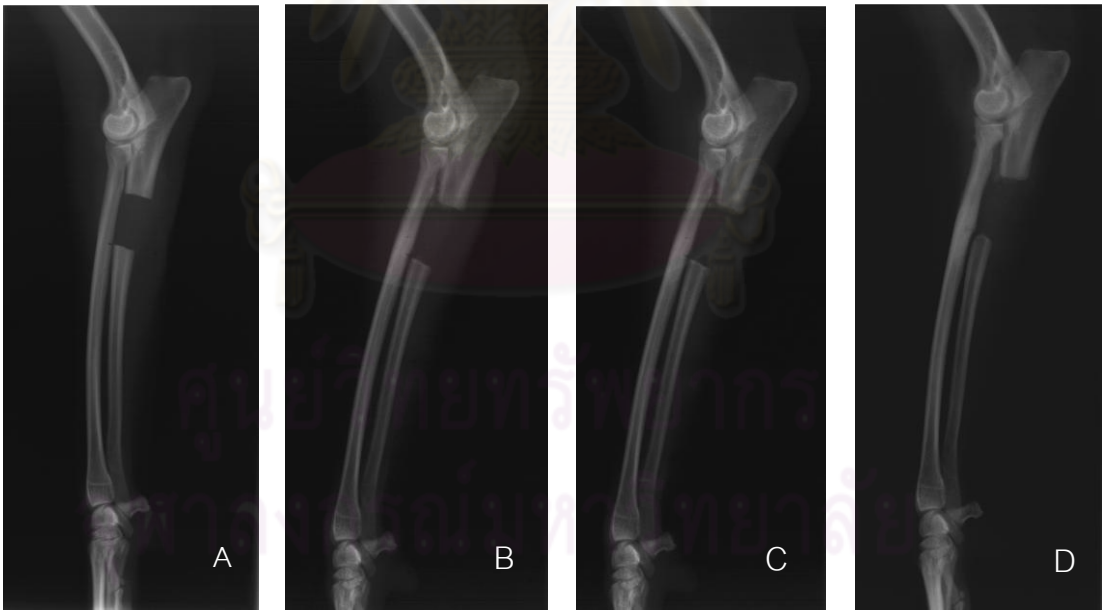

Figure 15 Radiographs of canine ulnar segmental defects treated with MSC-loaded PCL/HA scaffold at (A) 2 weeks; (B) 4 weeks; (C) 6 weeks and (D) 8 weeks postoperatively

Histological evaluation

Histopathology of the defect implanted with autogenous cancellous bone graft (group 1) showed a good incorporation between the graft and host bone (Figure 16A) with the osteoid formation and new bone formation along the graft-host bone junction. The longitudinal section of the graft revealed the re-establishment of vascular supply within the marrow cavity (Figure 16B). In group 2, the incorporation of the PCL/HA scaffold and host bone was mainly achieved by fibrocartilaginous tissue with minimal osteoid formation (Figure 17A). The defect site was filled with loose and unorganized connective tissue with new vascular ingrowth. There were still some remnants of the scaffold which sloughed off during the histological preparation (Figure 17B). Finally, in group 3, more fibrovascular tissue was observed in the defect, which implanted with MSC-loaded PCL/HA scaffold compared with PCL/HA group (Figure 18). The fibrous tissue is mainly comprised of spindle-shaped cells with extensive collagen deposition confirmed by Masson's Trichrome staining (Figure 19). It is notable that numerous of multinucleated giant cells were found adjacent to remnants of the scaffold indicating a chronic inflammation with foreign body giant cell response to the scaffold (Figure 20).

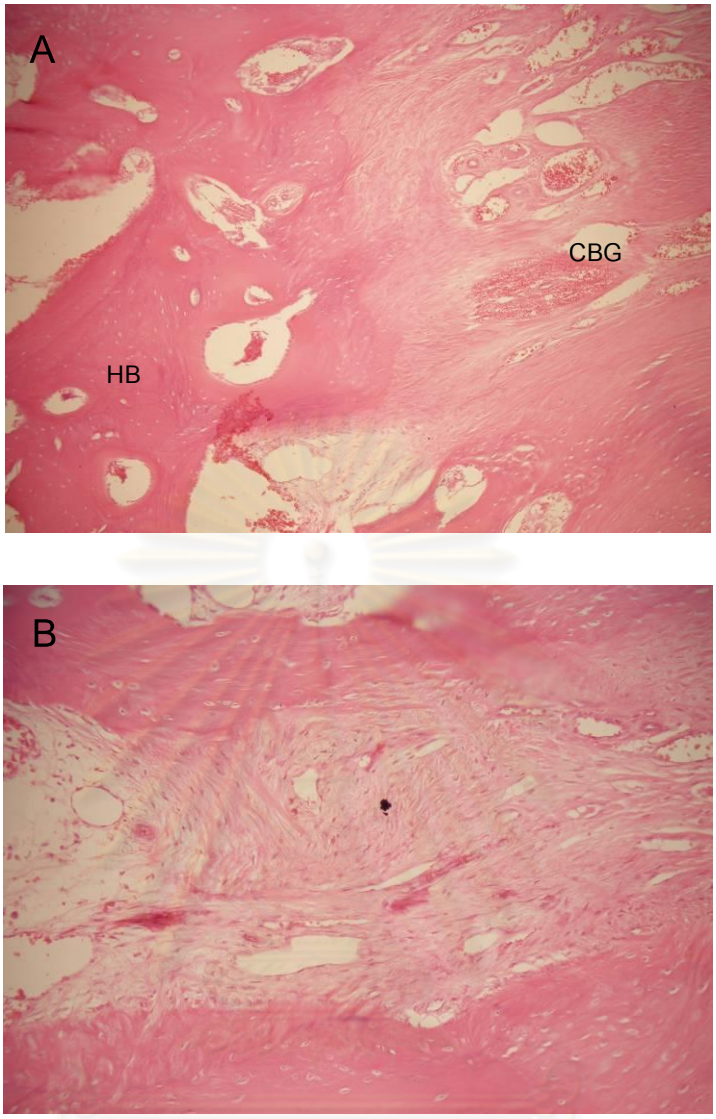

Figure 16 Histological sections of an ulnar defect implanted with cancellous bone graft (CBG) at 8 week postoperatively. A: At the junction between host bone (HB) and the graft. B: Longitudinal section of the corticocancellous bone graft

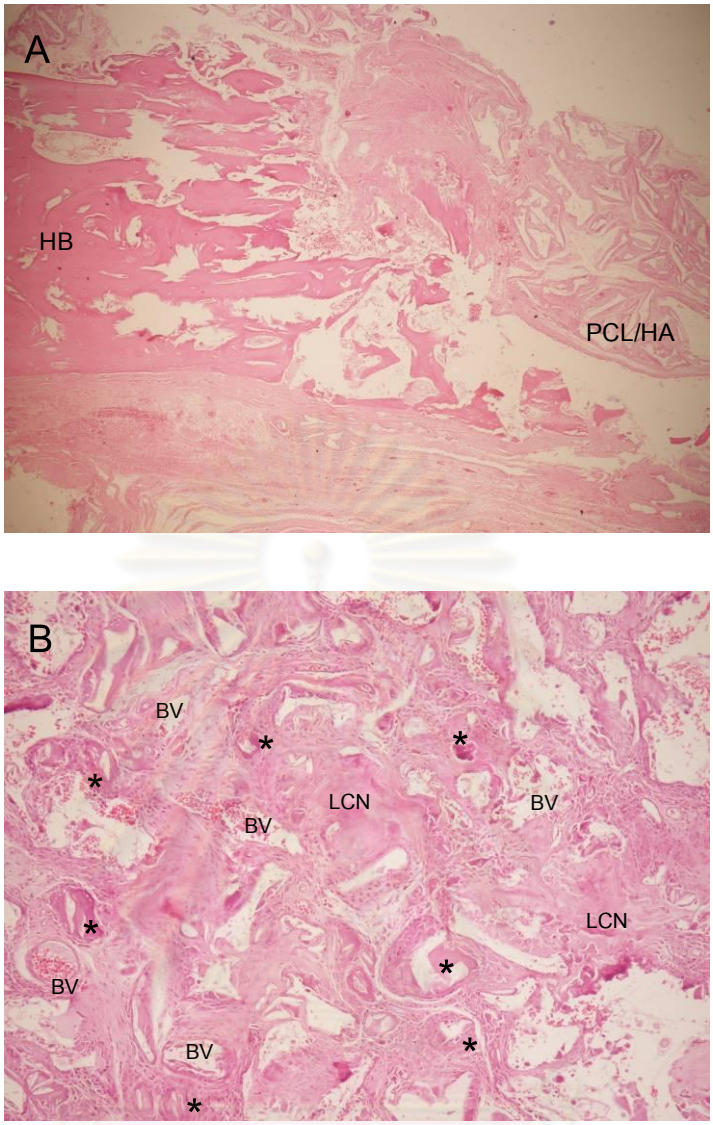

Figure 17 Histological sections of an ulnar defect implanted with PCL/HA scaffold at 8 week postoperatively. A: At the junction between host bone (HB) and PCL/HA scaffold. B: Cross sectional of the defect received PCL/HA scaffold (BV, new blood vessel; LCN, loose connective tissue; *, multinucleated giant cell)

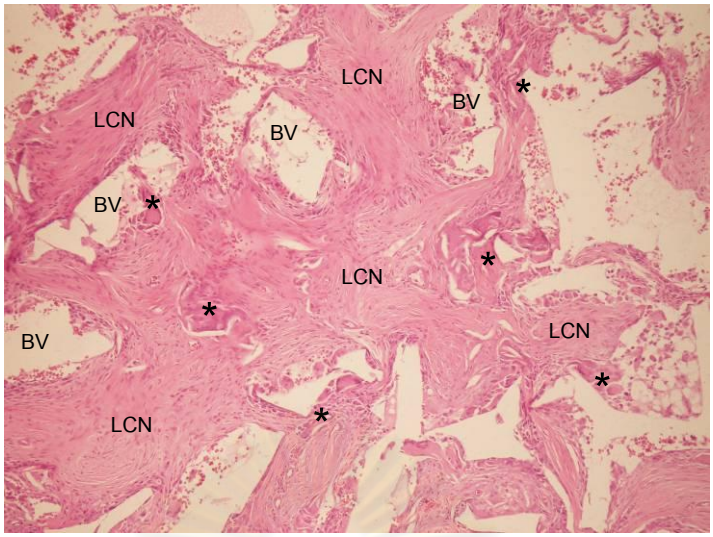

Figure 18 Histological sections of an ulnar defect implanted with MSC-loaded PCL/HA scaffold at 8 week postoperatively. (BV, new blood vessel; LCN, loose connective tissue; *, multinucleated giant cell)

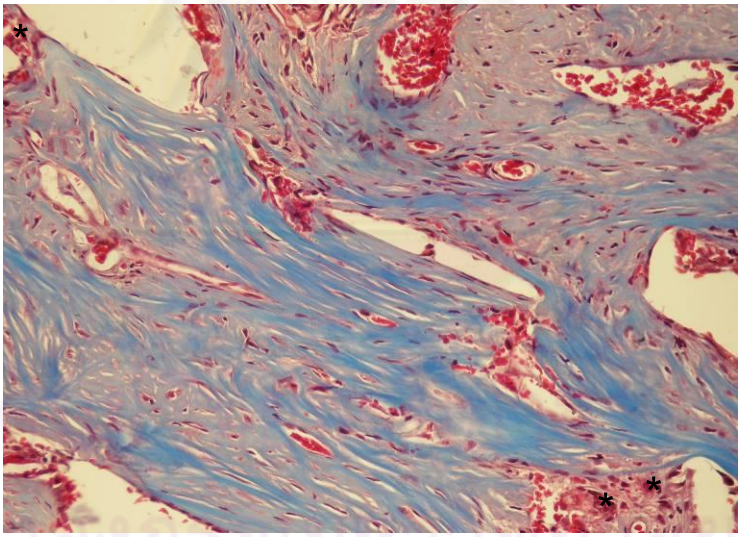

Figure 19 Histological section (hematoxylin and eosin (H&E) and Masson's trichrome staining) of ulnar defect implanted with MSC-loaded PCL/HA scaffold at 8 week postoperatively. (*, multinucleated giant cell)

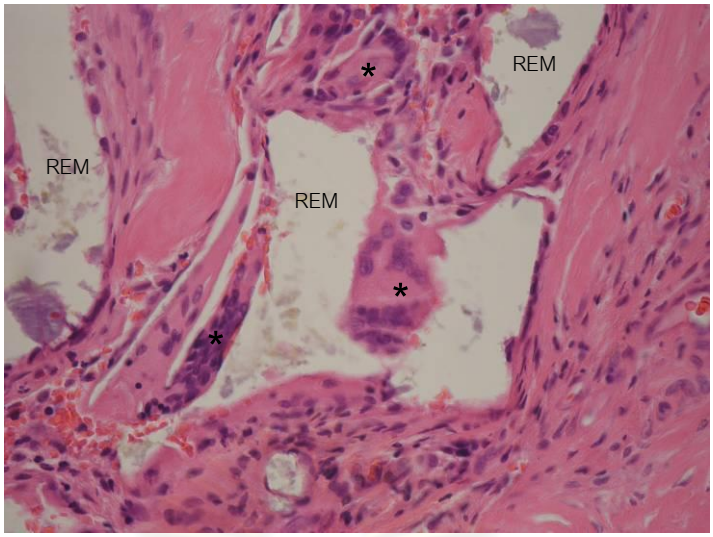

Figure 20 Numerous of multinucleated giant cells were found together with remnants of the PCL/HA. (*, multinucleated giant cell, REM, remnants of PCL/HA scaffold).

CHAPTER 5

CONCLUSION AND DISCUSSION

Conclusion

The present study was conducted in order to investigate the *in vitro* interaction between canine MSCs and PCL/HA composite scaffolds by seeding cells onto the scaffold and observed for cell behaviors with respect to cell viability, cell attachment and morphology, the proliferative capacity and the ability to differentiate into osteogenic lineage. The *in vitro* study demonstrated a good biocompatibility between canine MSCs and PCL/HA scaffolds. From dual fluorescence viability assay showed that the majority of seeded cells emitted green fluorescence indicating most of cells remained viable on day 1 after seeding. Similarly the result from SEM analysis revealed that canine MSCs adhered favorably onto PCL/HA scaffold. Cells already attached on the scaffold with flat morphology and filopodia projection within day 1 of seeding. More cell numbers were observed with formation of cell cluster in some area of scaffold suggested that canine MSCs were able to growth and maturation after seeding. To confirm the proliferative capacity of the seeded cell, serial DAPI florescent image analysis combined with BCA protein assay were performed. A progressive increase in DAPI-stained cells was observed under a fluorescent microscope on day 1, 2 and 4 after seeding which collated to an increase in total protein concentration on day 1 (523.33±15.27), day 3 (626.67±71.12) and day 5 (861.67±127.16) after seeding. Moreover, a significant increase ($p<0.05$) in protein concentration was observed between day 1 and 5 and day 3 and 5 of seeding. And finally, the ability of canine MSCs to differentiate into osteoblats were confirmed by Alizarin Red staining on day 14 of osteogenic induction. The present *in vitro* study concluded that there was a good interaction between canine MSCs and PCL/HA scaffold.

Despite a promising result from an *in vitro* study, neither bone nor callus formation was observed in canine ulnar defects that implanted with PCL/HA and PCL/HA scaffolds. Defects in these two groups were healed with fibrovascular tissue which

infiltrated through the pore of the scaffold. Surprisingly, numerous of multinucleated giant cells were found indicating chronic inflammation with foreign body giant cell response due to the presence of remnants of PCL/HA scaffold.

Discussion

Implantation of biological bone substitutes is one of the promising bone tissue engineering strategies for treatment of extensive bone defects. Mesenchymal stem cell in combination with polymer/ceramic composite scaffold has been widely investigated as an alternative to autogenous cancellous bone graft. In this study, we successfully isolated canine MSCs from bone marrow and identified these cells according to the multipotent human MSCs characterization which recently proposed by International Society for Cellular Therapy (Dominici et al., 2006). Then, we investigated the interaction between canine MSCs and PCL/HA composite scaffold in terms of cell viability, proliferative capacity and ability to differentiate into osteoblast. Finally, we evaluated the efficacy of canine MSCs combined with PCL/HA composite scaffold in comparison with PCL/HA alone and autogenous on the healing of ulnar critical sized defects in dog.

MSCs reside in various adult tissues such as bone marrow, adipose tissue, skin, periosteum and placenta (Tuan et al., 2002). These cells are responsible for regulating tissue homeostasis, repair and regeneration. Although MSCs originated from various tissue sources possess similar phenotypic expression, significant difference in cell proliferation and multilineage differentiation potentials are observed. In this study, bone marrow was chosen as a source of MSCs because it is easy to assess and can be aspirated in large volume. Moreover, MSCs derived from bone marrow and synovium are superior to periosteum-, adipogenic- and skeletal muscle- derived MSCs with regard to self renewal, expansion and differentiation potential (Sakaguchi et al., 2005). Canine MSCs were harvested from the bone marrow samples aspirated from the dorsal iliac crest of 4 dogs. Red blood cell lysing buffer was added to enrich the initial MSC population by eliminating the contaminated red blood cells before culture. Canine MSCs used in the present study were isolated by their ability to adhere to the polystyrene plastic plate and subsequently subcultured when cells reached 80-90% confluence. Owing to the absence of MSC specific antigen marker, at least three minimum criteria were required to characterize MSCs are as follows: the ability to adhere to plastic

surface, the expression of cell surface antigen and the capacity to differentiate along the mesenchymal lineage (Dominici et al., 2006). The isolated cells exhibited classical spindle shaped morphology and expressed high levels of MSC markers inculding CD 44 and CD 90. The flow cytometric analysis of cell surface protein revealed more than 94% of the isolated cells were positive for both CD 44 and CD 90 which corresponding with previous study (Kern et al., 2006; Jung et al., 2008). No expression of CD34 was observed which indicated no contamination of hematopoietic stem cells was found in the culture. And finally, these isolated cells were capable of differentiation into a mesenchymal lineage when cultured in a proper condition.

Due to the major concern in the survival and proliferative capacity of cells within the large scaffold constructs, an *in vitro* study of canine MSCs behavior was performed on 3D PCL/HA scaffolds. Dual fluorescence viability assay using calcein AM and ethidium homodimer was performed to determine the MSC viability within PCL/HA scaffold. This assay allows the simultaneous visualization of viable and dead cells within the scaffold (Decherchi et al., 1997). Calcein AM is a hydrophobic compound which can diffuse through intact cell membrane of viable cells and subsequently hydrolyze intracellular esterase result in calcein, a green fluorescence, retained in the cytoplasm. In contrast to calcein AM, ethidium homodimer can penetrate only damaged cell membranes and bind to DNA of the dead cells result in emission of red fluorescence. From dual viability assay, an intense green fluorescence was mainly observed through the entire scaffold indicated the majority of canine MSCs remained viable on day 1 after seeding. A small number of dead cells were found in the outer part of the scaffold and became more prominent in the middle of the scaffold. This may be due to the diffuse limitation of oxygen and nutrient caused by the scaffold thickness. Moreover, all MSC loaded-scaffolds were cultured under a static condition may even hinder the fluid transportation result in an accumulation of waste products within the scaffold. To overcome these problems, dynamic culture conditions such as a spinner flask, orbital shaker or perfusion system has been used since the approach can improve cell viability, uniform distribution and subsequently increase in extracellular matrix deposition (Yeatts and Fisher, 2011). Nerurkar et al. (2011) suggested that the dynamic culture condition using orbital shaker enhanced MSC infiltration and collagen deposition on electrospun

PCL nanofibrous scaffold. Additionally, transient shaking culture significantly improved MSC distribution, provided favorable condition for chondrogenic differentiation and increased glycosaminoglycans accumulation within the scaffold.

The results from SEM images showed that canine MCSs adhered favorably to PCL/HA scaffold. Cells exhibited flat morphology with filopodia projected from cell body and attached to the scaffold surface. Filopodia are protrusion of cell membrane which play an important role in the formation of adhesive connection between cell and the extracellular matrix (Yang et al., 2010). The attached cells became more elongated in shaped with an enlargement of focal adhesion suggested growth and maturation of canine MSCs in PCL/HA scaffold over time. MSC proliferative capacity on 3D PCL/HA scaffold was evidenced by comparison of serial DAPI fluorescence images. DAPI is a DNA-specific dye which has been commonly used for DNA detection and visualization. This dye binds specifically to A-T base pair in DNA sequence results in formation of the DAPI-DNA complex which exhibits a blue fluorescence emission under a fluorescence microscope. An increase in DAPI stained nuclei was observed over time reflected the proliferative capacity of the loaded MSCs. Notably, the background interference was observed during the fluorescent microscopical analysis of the loaded scaffold in both dual viability assay and DAPI fluorescent staining. It is thought that the autofluorescence emission of the polymers caused by an aromatic and aliphatic ester bond when excited with green or blue wavelength. Moreover, the fluorescent interference is even more exaggerated due to the light scattering caused by the thickness of the polymer and its porous nature. To avoid these interferences, a thin section of the sample can diminish light scattering and minimize over all autofluorescence from polymer or using other fluorescent probe that can be excited and emits in the different wavelength. Jaafar et al. (2011) applied the use of Sudan Black B (SB) as an autofluorescence quencher for 4 types of polymer, including polyglycerol sebacate, polyurethane, polylactice-co-caprolactone, and polylactic acid-co-glycolic acid. SB is a lysochrome diazo dye which has been commonly used as a neutral triglyceride and lipid staining. Reduction of an overall background interference was based on two mechanisms, the light absorption capacity of SB and the ability to modify the surface of the polymers. No interaction between SB and fluorescently labeled cells was observed.

Despite the promising result from the visual DAPI fluorescence image analysis, the uncertainty of the outcome may occur due to the subjective evaluation of these images. Therefore, the BCA protein assay was performed in order to quantify proliferative capacity of canine MSCs after seeded onto the scaffold (Sachana and Hargreaves, 2007). The assay is based on the ability of the peptide bonds in protein to reduce Cu^{+2} into Cu^{+1} and the chelation of Cu^{+1} with BCA result in purple-colored products that can be measured with spectrophotometer. The total protein concentration are calculated from the optical density of each the samples at a wavelength of 562 nm with respect to the standard curve. Significant increases in the protein concentration were observed between day 1 and day 5 and day 3 and day 5 ($p<0.05$). An increase in the absorbance of the loaded PCL/HA is correlated with the greater amount of the protein concentration in the sample indicated the growth and proliferative capacity of canine MSCs resided in the scaffold. As expected, there was no significant difference in protein concentration was found between day 1 and day 3. These may result from the physical adaptation of cells to the change in environment. Moreover, the newly seeded cells may also require time to adjust and adhere onto the new surface condition and subsequently reformation of the intercellular connection which necessary for optimal cell proliferation. And finally, the present *in vitro* study demonstrated the ability of canine MSCs to differentiate into an osteogenic lineage after seeded onto 3D PCL/HA scaffold as evidenced by Alizarin staining on day 14 of induction.

As the combination of osteopotential cell and biolodegradable scaffold is one of the most successful strategies in bone tissue engineering and the use of PLC/HA composite scaffold fabricated by solvent casting and particular leaching techniques has been demonstrated as a promising approach for promoting new bone formation (Chuenjitkuntaworn et al., 2010). This study was performed as a further investigation using canine model in order to evaluate the efficacy of PCL/HA and MSC-loaded PCL/HA on the healing of ulnar critical size defects. Key (1934) has defined the ulnar critical sized defect as a segmental defect that larger than 1 to 1.5 times of the diameter of the shaft of the bone. All dogs were able to stand and ambulate on day 1 and 2 after surgery, respectively. Defects in PCL/HA group were healed with fibrous connective tissue consisted of long spindle-shaped fibroblastic cells and collagen fiber as an

extracellular matrix. The presence of capillaries within the graft sites suggested that PCL/HA scaffolds can support the ingrowth of vascular tissue. Similar results were obtained in the group that treated with MSC-loaded PCL/HA scaffold, however, Mason's trichrome staining suggested that more collagen deposition was found when compared to PCL/HA group. Although there was a good evidence of fibrovascular tissue infiltration with an extent matrix deposition throughout the entire PCL/HA scaffold, no osteogenic differentiation was observed. In contrast to the promising result in a calvarial defect of mouse (Chuenjitkuntaworn et al., 2010) neither new bone nor callus formation was observed in defects treated with PCL/HA alone or MSC-loaded PCL/HA scaffold. Several possible reasons could explain for this inconsistency. It is believed that larger animal possesses bone regenerative capacity to a lesser extent than small animal. Moreover, the physiological differences between dog and mouse with regard to the slower bone turnover rate lower basal metabolic rate and longer lifespan in dog may contribute to different bone healing result (Cook et. al., 1994). The variation in size, location and the mechanical environment of the defects may impact on the biological response to the scaffold. PCL/HA scaffolds used in the present study were not only larger in size but also thicker in dimension than the previous study. This may cause a massive release of the degradation product, caproic acid, from the scaffold and subsequently creating an unfavorable environment for bone regeneration (Böstmann et al. 1990; Bergsma et al., 1995; Prokop et al., 2004). And finally, the major consideration was given to the different types of bone defect (flat bone versus long bone), the loading condition of the bone (non-loading calvarial versus loading ulnar bone). A calvarial defect is considered as a non-weight-bearing model which experiences lesser mechanical interference than a long bone model. Therefore, a calvarial bone defect may provide more favorable environment for new bone regeneration than an ulnar bone defect in a biomechanical aspects.

Canine ulna defect model has been extensively used as a study model to evaluate the efficacy of biomaterials in bone tissue engineering application because no fixation is required as the radius is the major load-bearing bone of the forearm and the interosseous ligament between the radius and the ulna was remained intact. Moreover, the ulnar ostectomy procedure can be done on both sides simultaneously, thus

reducing the number of animal used in the study (Salkeld et al., 2001; Paskalev et al., 2006; Jones et al., 2008). Several successful results have been reported using a canine ulnar model without fixation (Heiple et al., 1963; Nillson et. al., 1986; Cook et al., 1994; Salkeld et al., 2001; Paskalev et al., 2006; Jones et al., 2008). However, there might be some mechanical interference between defect sites causing an unfavorable condition for mesenchymal stem cells to differentiate into osteoblastic cells. To overcome this problem, intramedullary pins or plates and screws may use to stabilize canine ulnar defect in order to optimize the new bone formation.

Last but not least, histological analysis demonstrated the presence of numerous multinucleated giant cells within defect sites that implanted with PCL/HA and MSC-loaded PCL/HA scaffold. These giant cells appeared adjacent to remnants of the scaffold which reflected chronic inflammation with foreign body response. For this reason, scaffold samples were sent to identify the contamination using scanning electron microscope with energy dispersive x-ray (SEM/EDX) analysis. The result of the SEM/EDX analysis showed that the scaffolds were contaminated with copper (Cu) from hydroxyapatite ceramic. Thus, chronic inflammation with foreign body giant cell response from copper contamination may result in an impaired new bone formation at defect site. Similar tissue reaction was reported by Linder and Lundskog (1975), Völker et al. (1997), Tindel et al. (2001) and Saitoh et al. (2010). Saitoh and his group investigated an in vivo tissue response to three different metal particles including copper, nickel and titanium by subcutaneous implantation in mouse. One week after implantation, subcutaneous tissue was excised for evaluation of tissue reaction using histological and transmission electron microscopic analysis. The result of this study showed that copper particles caused the highest degree of inflammation. Similar result was observed in the study of Linder and Lundskog that compared the reaction of bone to copper, stainless steel, titanium and vitallium.

References

Amato, H., Ciapetti, G., Pagani, S., Marletta, G., Satriano, C., Baldini, N. and Granchi, D. 2007. Expression of cell adhesion receptors in human osteoblasts cultured on biofunctionalized poly-(ε-caprolactone) surfaces. Biomaterials 28: 3668-3678.

Azevedo, M. C., Reis, R. L., Claase, M. B., Grijpma, D. W. and Feijen. J. 2003. Development and properties of polycaprolactone/hydroxyapatite composite biomaterials. J. Mater. Sci. Mater. Med. 14(2): 103-107.

Ashton, B. A., Allen, T. D., Howlett, C. R., Eaglesom, C. C., Hattori, A. and Owen, M. 1980. Formation of bone and cartilage by marrow stromal cells in diffusion chambers *in vivo*. Clin. Orthop. 151: 294-307.

Bergsma, E. J., Rozema, F. R., Bos, R. M. and Brujn, W. 1993. Foreign body reactions to resorbable poly(L-lactide) bone plate and screws used for the fixation of unstable zygomztic fractures. J. Maxillofac. Surg. 51: 666-670.

Bosch, P., Pratt, S.L. and Stice, S.L. 2006. Isolation, characterization, gene modification, and nuclear reprogramming of porcine mesenchymal stem cells. Biol Reprod.74: 46-57.

Böstmann, O., Hirvensalo, E., Mäkinen, J. and Rokkanen, P. 1990. Foreign body reactions to fracture fixation implants of biodegradable synthetic polymers. J. Bone Jt. Surg. B72:592.

Breuls, R. G. M., Jiya, T. U. and Smit, T. H. 2008. Scaffold stiffness influences cell behavior: opportunities for skeletal tissue engineering. Open Orthop. J. 2: 103-109.

Bunnel, B. A., Flaat, M., Gagliardu, C., Patel, B. and Ripoll, C. 2007. Adipose-derived stem cells: Isolation, expansion and differentiation. Bull. Exp. Biol. Med. 140(1): 138-143.

Calandrelli, L., Immirzi, B., Malinconico, M. and Luessenheide, S. 2004. Natural and synthetic hydroxyapatite filled PCL: mechanical properties and biocompatibility analysis. J. Bioact. Compat. Polym. 19: 301-313.

Ciapetti, G., Ambrosio, L., Savarino, L., Granchi, D., Cenni, E., Baldini, N., Pagani, S., Guizzardi, S., Causa, F. and Guinti, A. 2003. Osteoblast growth and function in porous poly ε-caprolactone matrices for bone repair: a preliminary study. Biomaterial. 24: 3815-3824.

Chen, B. and Sun, K. 2005. Mechanical and dynamic viscoelastic properties of hydroxyapatite reinforced poly(ε-caprolactone). Polym. Test. 24: 978-982.

Chuenjitkuntaworn, B., Inrung, W., Mekaapiruk, K., Damrongsri, D., Supaphol, P. and Pavasant, P. 2010. Polycaprolactone/hydroxyapatite composite scaffolds: preparation, characterization and in vitro and in vivo biological responses of human primary bone cells. J. Biomed. Mat. Res. A 94(1): 241-251.

Cook, S. D., Baffes, G .C, Wolfe, M. W., Sampath, T. K. and Rueger, D. C. 1994. Recombinant human bone morphogenetic protein-7 induces healing in a canine long-bone segmental defect model. Clin. Orthop. Related Res. 301: 302-312.

Cornell, C. N. 1999. Osteoconductive materials and their role as substitutes for autogenous bone grafts. Orthop. Clin. North Am. 30: 592-600.

Decherchi, P, Cochard, P. and Gauthier, P. 1997. Dual staining assessment of Schwann cell viability within whole peripheral nerves using calcein-AM and ethidium homodimer. J. Neurosci. Meth. 71: 205–213.

Dickson, G., Buchsnan, F., Marsh, D., Harkin-Jones, E., Little, U. and McCaigue, M. 2007. Orthopedic tissue engineering and bone regeneration. Technology and Health Care 15: 57-67.

Dominici, M., Le Blanc, K., Mueller, I., Slaper-Cortenbach, I., Marini, F. C. Krause, D. S., Deans, R. J., Keating, A., Prockop D. J. and Horwitz, E. M. (2006) Minimal criteria for defining multipotent mesenchymal stromal cells. The International Society for Cellular Therapy position statement. Cytotherapy 8(4): 315-317.

Drosse, I., Volkmer, E., Capanna, R., Biase, P. D., Mutschler, W. and Schieker, M. 2008. Tissue engineering for bone defect healing: An update on a multi-component approach. Injury, Int. J. care Injured 39S2: S9-S20.

Dupont, K. M., Sharma, K., Stevens, H. Y., Boerckel, J D., Garcia, A. J. and Guldberg, R. E. 2010. Human stem cell delivery for treatment of large segmental bone defects. Proceedings of the National Academy of Sciences 107(8): 3305-3310.

Fabbri, P., Bondioli, F., Messori, M., Baetoli, C., Dinucci, D. and Chillini, F. 2010. Porous scaffolds of polycaprolactone reinforced with *in situ* generated hydroxyapatite for bone tissue engineering. J. Mater. Sci. Mater. Med. 21(1): 343-351.

Jaafar I. H., LeBlon, C. E., Wei, M., Ou-Yang, D. and Coulter, L. P. 2011. Improving fluorescence imaging of biological cells on biochemical polymers. Acta Biomat. 7: 1588-1598.

Giancotti, F. G. 1999. Integrin signaling. Science 285: 1028-1032.

Griffon, D. J. 2005. Fracture healing. In A. L. Johnson, J. E. F. Houlton and R. Vannini (eds.), AO Principles of fracture management in the dog and cat, pp.73-98. Davos Platz, Switzerland. AO publishing.

Guarino, V., Causa, F., Taddei, P., di Foggia, M., Ciapetti, G., Martini, D., Fagnano, C., Baldini, N. and Ambrosio, L. 2008. Polylactic acid fibre-reinforced polycaprolactone scaffolds for bone tissue engineering. Biomater. 29(27): 3662-3670.

Gunatillake, P. A. and Adhikari, R. 2003. Biodegradable synthetic polymers for tissue engineering. Eur. Cells Mater. 5:1-16.

Heiple, K. G., Chase, S. W. and Herdon, C. H. 1963. A comparative study of the healing process following different types of bone transplantation. J. Bone Joint Surg. Am. 45:1593-1616.

Heng, B. C., Bezerra, P. P., Meng, Q. R., Chin, D. W., Koh, L. B., Zhang, H., Preiser, P. R., Boey, F. Y. and Venkatraman, S. S. 2010. Adhesion, proliferation, and gene expression profile of human umbilical vein endothelial cells cultured on bilayered polyelectrolyte coatings composed of glycosaminoglycans. Biointer. Phases 5(3): 53-62.

Heo, S. J., Kim, S. E., Hyun, Y. T., Kim, D. H., Lee, H. M., Shin, J. W., Hwang, Y. M. and Shin, J. W. 2007. Biodegradable composite of poly ε-caprolactone/ hydroxyapatite 3-D scaffolds for bone tissue engineering. In F. Ibrahim, N. A. Abu Osman, J. Usman and N. A. Kadri (eds.), Proceedings of the International Federation for Medical and Biological Engineering, pp. 672-675. Berlin: Springer.

Hulbert, S. F., Young, F. A. and Mathews, R. S. 1970. Potential of ceramic materials as permanently implantable skeletal prostheses. J. Biomed. Mater. Res. 4(3): 433-456.

Hutmacher, D. W. 2000. Scaffolds in tissue engineering bone and cartilage. Biomaterials. 21: 2529-2543.

Hutmacher, D. W., Schantz, J. T., Lam, C. X. F., Tan, K. C. and Lim, T. C. 2007. State of the art and future directions of scaffold-based bone engineering from a biomaterials perspective. J. Tissue Eng. Regen. Med. 1: 245-260.

Jones, C. B., Sabatino, C. T., Badura, J. M., Sietsema, D. L. and Marotta, J. S. 2008. Improved healing efficacy in canine ulnar segmental defects with increasing recombinant human bone morphogenetic protein-2/allograft ratios. J. Orthop. Trauma. 22(8): 550-559.

Karageorgiou, V. and Kaplan, D. 2005. Porosity of 3D biomaterial scaffolds and osteogensis. Biomaterials 26: 5474-5491.

Keating, J. F. and McQueen, M. M. 2001. Substitutes for autogenous bone graft in orthopaedic trauma. J. Bone Joint Surg. Br. 82-B: 3-8.

Kern, S., Eichler, H., Stoeve, J., Klüter, H. and Bieback, K. 2006. Comparative analysis of mesenchymal stem cells from bone marrow, umbilical cord blood, or adipose tissue. Stem cells 24: 1294-1301.

Key, J. A. 1934. The effect of a local calcium depot on osteogenesis and healing of fractures. J. Bone Joint Surg. Am. 16: 176-184.

Khan, Y., Yaszemski, M. J., Miko, A. G. and Laurencin, C. T. 2008. Tissue engineering of bone: Material and matrix consideration. J. Bone Joint Surg. Am. 90: 36-42.

Kraus, K. H. and Kirker-head, C. 2006. Mesenchymal stem cell and bone regeneration. Vet . Surg. 35: 232-242.

Kuboki, Y., Takita, H., Kobayashi, D., Tsuruga, E., Inoue, M., Murata, M., Nagai, M., Dohi, N. and Ogushi, H. 1998. BMP-induced osteogensis on the surface of hydroxyapatite with geometrically feasible and nonfeasible structures: topology of osteogensis. J. Biomed. Mater. Res. 39(2): 190-199.

Langer, R. and Vacanti, J. P. 1993. Tissue engineering. Science. 260: 920-926.

Lui, X. and Ma, X. 2004. Polymeric scaffolds for bone tissue engineering. Ann. Biomed. Eng. 32(3): 477-486.

Martin, D. R., Cox, N. R., Hathcock, T. L., Neimeyer, G. P. and Baker, H. J. 2002. Isolation and characterization of multipotential mesenchymal stem cells from feline bone marrow. Exp. Hematol. 30(8): 879-886.

Martinez, S. A. and Walker, T. 1999. Bone graft. Vet. Clin. North Ame. Small Ani. Pract. 29(5): 1207-1213.

Meyer, U. and Wiesmann, H. P. 2006. Bone and Cartilage Engineering. Berlin: Springer.

Miao, Z., Jin, J., Chen, L., Zhu, J., Huang, W., Zhao, J., Qian, H. and Zhang, X. 2006. Isolation of mesenchymal stem cells from human placenta: Comparison with human bone marrow mesenchymal stem cells. Cell Biol. Int. 30: 681-687.

Mistry, A. S. and Mikos, A. G. 2005. Tissue engineering strategies for bone regeneration. Adv. Biochem. Engin./Biotechnol. 94: 1-22.

Moore, W. R., Graves, S. E. and Bain, G. I. 2001. Synthetic bone graft substitutes. ANZ. J. Surg. 71: 354-361.

Mygind, T., Stiehler, M., Baatrup, A., Li, H., Zou, X., Flyvbjerg, A., Kassem, M. and Bünger, C. 2007. Mesenchymal stem cell ingrowth and differentiation on coralline hydroxyapatite scaffolds. Biomaterials 28: 1036-1047.

Nilsson, O. S., Urist, M. R., Dawson, E. G., Schmalzried, T. P. and Finerman, G. A. M. 1986. Bone repair induced by bone morphogenetic protein in ulnar defects in dogs. J. Bone Joint Surg. Br. 68(4): 635-642.

Necas, A., Planka, L., Srnec, R., Rauser, P., Urbanova, L., Lorenzova, J., Crha, M. Jancar, J. and Gal, P. 2008. Biomaterials and stem cells in the treatment of articular cartilage, meniscal, physeal, bone ligament and tendinous defects. Acta. Vet. Brno. 77: 277-284.

Nerurkar, N. L., Sen, S., Baker, B. M., Elliott, D. M. and Mauck, R. L. 2011. Dynamic culture enhances stem cell infiltration and modulates extracellular matrix production on aligned electrospun nanofibrous scaffolds. Acta Biomater. 7: 485-491.

Neuendorf, R. E., Saiz, E., Tomsia, A. P.and Ritchie, R. O. 2008. Adhesion between biodegradable polemers and hydroxyapatite: relevance to synthetic bone-like materials and tissue engineering scaffolds. Acta Biomater. 4(5): 1288-1296.

Oh, S., Oh, N., Appleford, M. and Ong, J. L. 2006. Bioceramics for tissue engineering applications – a review. Am. J. Biochem. Biotechnol. 2(2): 49-56.

Oh, S. H., Park, I. K., Kim, J. m. and Lee, J. H. 2007. In vitro and in vivo characteristics of PCL scaffolds with pore size gradient fabricated by a centrifugation method. Biomaterials. 28: 1664-1671.

Park, S. A., Lee, S. H. and Kim, W. D. 2010. Fabrication of porous polycaprolactone/hydroxyapatite (PCL/HA) blend scaffolds using a 3D plotting system for bone tissue engineering. Bioprocess. Biosyst. Eng. DOI: 10.1007/s00449-010-0499-2.

Paskalev, M., Krastev, S., Mechkarski, S. V., Philipov, J. and Dyakova, S. V. 2006. Experimental study on guided bone regeneration in canine segmental ulnar defects. Bulg. J. Vet. Med. 9(4): 281-291.

Pittenger, M. F., Mackay, A. M., Beck, S. C., Jaiswal, R. K., Douglas, R., Mosca, J. D., Moorman, M. A., Simonetti, W., Crgig, S. and Marshak, D. R. 1999. Multilineage potential of adult human mesenchymal stem cells. Science. 284:143-144.

Porter, J. R., Ruckh, T. T. and Popat, K. C. 2009. Bone tissue engineering: a review in bone biomimetics and drug delivery strategies. Biotechnol. Prog. 25(6): 1539-1560.

Prokop, A., Jubel, A., Helling, H. J., Eibach, T., Peters, C., Baldus, S. E. and Rehm, K. E. 2004. Soft tissue reactions of different biodegradable polylactide implants. Biomaterials 25: 259-267.

Rai, B., Ho, K. H., Lei, Y., Teo, C. J., Yacob, K. B., Chen, F. Ng, F. ans Teoh, S. H. 2007. Polycaprolactone-20% tricalcium phosphate scaffolds in combination with platelet-rich plasma for the treatment of critical-sized defects of the mandible: a pilot study. J. Oral Maxillofac. Surg. 65: 2195-2205.

Remedios, A. 1999. Bone and bone healing. 1999. Vet. Clin. North Am. Small Anim. Pract. 29(5): 1029-1044.

Rezwan, K., Chen, Q. Z., Blaker, J. J. and Boccaccini, A. B. 2006. Biodegradable and bioactive porous polymer/inorganic composite scaffolds for bone tissue engineering. Biomaterials 27: 3413-3431.

Roberts, S. J., Howard, D., Buttery, L. D. and Shakesheff, K. M. 2008. Clinical applications of musculoskeletal tissue engineering. British Medical Bulletin. 86: 7-22.

Rohner, D., Hutmacher, D., See, P., Cheng, T. K., Yeow, V., Yong, T. S., Teik, L. S. and Hammer, B. 2002. Reconstruction of craniofacial defects with bone-marrow-coated polycaprolactone scaffolds: an animal study in the Yorkshire pig. Proceedings of the 12th Singapore General Hospital Annual Scientific Meeting. 11(1): 32-39.

Rohner, D., Hutmacher, D., Cheng, T. K., Oberholzer, M. and Hammer, B. 2003. *In vivo* efficacy of bone-marrow-coated polycaprolactone scaffolds for the reconstruction of orbital defects in the pig. J. Biomed. Mater. Res. Part B: Appl. Biomater. 66B: 574-580.

Sachana, M. and Hargreaves, A. J. 2007. Toxicological testing: *in vivo* and *in vitro* Model. In: R. C. Gupta (ed.), Veterinary toxicology: basic and clinical principles. pp. 51-66. California. Elsevier.

Sachlos, E. and Czernuszka, J. T. 2003. Making tissue engineering scaffold work. Review on the application of solid freeform fabrication technology to the ptoduction of tissue engineering scaffolds. Eur. Cell and Mater. 5: 29-40.

Sakaguchi, Y., Sekiya, I., Yagishita, K., and Muneta, T. 2005. Comparison of human stem cells derived from various mesenchymal tissues. Arthritis Rheum. 52(8): 2521-2529.

Salgado, A. J., Gomes, M. E. and Reis, R. L. 2004. Tissue engineering of mineralized tissue: the essential element. In: Learning from nature how to design new implantable biomaterial. Dordrecht: Kluwer academic publishers. 205-222.

Salkeld, S. L., Patron, L. P., Barrack, R. L. and Cook S. D. 2001. The Effect of osteogenic Protein-1 on the healing of segmental bone defects treated with autograft or allograft bone. J. Bone Joint Surg. Am. 83-A (6): 803 – 816.

Samuelson, D. A. 2007. Cartilage and bone. In: T. Merchant (ed.), Textbook of veterinary histology, pp. 100-129. Missouri: Sauders.

Savarino, L., Baldini, N., Greco, M., Capitani, O., Pinna, S., Valentini, S., Lombrado, B., Esposito, M. T., Pastore, L., Ambrosio, L., Battista, S., Causa, F., Zeppetelli, S., Guarino, V. and Netti, P. A. 2007. The performance of poly-ε-caprolcatone scaffolds in a rabbit femur model with and without autologous stromal cells and BMP-4. Biomaterials 28: 3101-3109.

Schuckert, K. H., Joop, S. and Teoh, S. W. 2009. Mandibular defect reconstruction using three-dimensional polycaprolactone scaffold in combination with platelet-rich plasma and recombinant human bone morphogenetic protein-2: *De novo* synthesis of bone in a single case. Tissue Eng. Part A 15(3): 493-499.

Sfeir, C., Ho, L., Doll, B. A., Azari, K. and Hollinger, J. O. 2005. Fracture Healing. In: J. R. Lieberman and G. E. Friedlaender (eds.), Bone Regeneration and Repair, pp. 21-44. New Jersey: Humana.

Sharma, P., Cartmell, S. and El Haj A. J. 2005. Applications of Cell Immobilization Biotechnology. Dordrecht: Springer. 153-166.

Shor, L., Güceri, S., Wen, X., Gandhi, M. and Sun, W. 2007. Fabrication of three-dimensional polycaprolactone/hydroxyapatite tissue scaffolds and osteoblast-scaffold interactions in vitro. Biomaterials 28: 5291-5297.

Silvio, L. D., Dalby, M. J. and Bonfield, W. 2002. Osteoblast behavior on HA/PE composite surfaces with different HA volume. Biomaterials 23: 101-107.

Skarda, R. T. and Tranquilli, W. J. 2007. Local and regional anesthetic and analgesic techniques: dogs. In: W. J. Tranquilli, J. C. Thurmon and K. A. Grimm. (eds.), Lump and Jones' veterinary anesthesia and analgesia, 4th ed. pp. 561-594. Iowa: Blackwell.

Tabata. Y. 2009. Biomaterial technology for tissue engineering applications. J. R. Soc.: Interface. 6: S311-324.

Tondreau, T., Lagneaux, L., Dejeneffe, M., Delforge, A., Massy, M., Mortier, C. and Bron, D. 2004. Isolation of BM mesenchymal stem cells by plastic adhesion or negative selection: phenotype, proliferation kinetics and differentiation potential. Cytotherapy 6(4): 372- 379.

Toma, J, G., Akhavan, M., Femandes, K. J. L., Barnabé-Heider, F., Scdikot, A., Kaplan, D. R. and Miller, F. D. 2001. Isolation of multipotent adult stem cells from the dermis of mammalian skin. Nature cell biol. 3: 778-784.

Tuan, R. S., Boland, G. and Tuli, R. 2002. Adult mesenchymal stem cells and cell-based tissue engineering. Arthr. Res. Ther. 5(1): 32-45.

Van den Bogert, C., Van Kernebeek, G., Leij, L. D. and Kroom,. 1986. Inhibition of mitochondrial protein synthesis leads to proliferation arrest in the G_1-phase of the cell cycle. Cancer Lett. 32(1): 41-5.

Wang, M. 2006. Composite scaffolds for bone tissue engineering. Am. J. Biochem. Biotechnol. 2(2): 80-84.

Williams, J. M., Adewunmi, A., Schek, R. M., Flanagan, C. L., Krebsbach, P. H., Feinberg, S. E., Hollister, S. J. and Das, S. 2005. Bone tissue engineering using polycaprolactone scaffolds fabricated via selective laser sintering. Biomaterials 26: 4817-4827.

Wexler, S. A., Donaldson, C., Denning-Kendall P., Rice, C., Bradley, B. and Hows, J. M. 2003. Adult bone marrow is a rich source of human mesenchymal “stem” cells but umbilical cord and mobilized adult blood are not. Br. J, Haemato. 121: 368-374.

Wutticharoenmongkol, P., Sanchavanakit, N., Pavasant, P. and Supaphol, Pitt. 2006. Novel bone scaffolds of electrospun polycaprolactone fibers filled with nanoparticles. J. nanosci. Nanotechnol. 6: 514-522.

Wutticharoenmongkol, P., Pavasant, P. and Supaphol, P. 2007. Osteoblast phenotype expression of MC3T3-E1 cultured on electrospun polycaprolactone fiber mats filled with hydroxyapatite nanoparticles. Biomacromolecules. 8: 2602-2610.

Yang, C., Huang, L., Shen, T. and Yeh, J. A. 2010. Cell adhesion, morphology and biochemistry on nanotopographic oxidized silicon surface. Eur. Cell Mater. 20: 415-430.

Yeatts, A. B. and Fisher, J. P. 2011. Bone tissue engineering bioreactors: dynamic culture and the influence of shear stress. Bone. 48(2): 171-181.

Yu, H., Wooley, P. H. and Yang, S. 2009. Biocompatibility of polycaprolactone-hydroxyapatite composite on mouse bone marrow-derived osteoblasts and endothelail cells. J. Orthop. Res. 4: 5-13.

Appendix

Table 6 Radiographic scores of defects implanted with autogenous corticocancellous graft (group 1)

2 weeks	4 weeks	6 weeks	8 weeks
2	0	4	4
1	1	2	4
2	3	1	3
0	3	4	4
0	2	2	2
1	3	2	2
0	1	4	4
0	0	4	1
0	2	3	3
1	4	3	5
1	2	1	5
1	2	1	5

Table 7 Radiographic scores of defects implanted with PCL/HA scaffolds (group 2)

2 weeks	4 weeks	6 weeks	8 weeks
1	1	1	1
1	0	1	2
2	0	0	1
1	2	1	1
0	1	2	1
2	2	2	2
1	3	1	2
1	2	1	1
1	3	1	3
1	0	2	1
1	1	1	2
1	0	3	1

Table 8 Radiographic scores of defects implanted with MSC-loaded PCL/HA scaffolds (group 3)

2 weeks	4 weeks	6 weeks	8 weeks
0	2	1	1
0	1	0	1
0	2	1	2
2	1	1	1
2	1	0	1
2	1	0	2
0	1	1	1
0	2	0	1
1	1	1	2
0	1	1	1
0	2	0	1
1	1	1	2

Biography

Miss Sasijaras Tantrajak was born on 8 September 1984 in Bangkok. She got her bachelor degree, Doctor of Veterinary Medicine (2nd Class Honors), from Faculty of Veterinary Science, Chulalongkorn University in academic year 2007. After that she has enrolled in the Degree of Master science of Science Program in Veterinary Surgery since academic year 2008.